中国科学: 地球科学 2020 年 第 50 卷 第 12 期: 1818 ~ 1844
SCIENTIA SINICA Terrae earthcn.scichina.com
《中国科学》杂志社 SCIENCE CHINA PRESS

综 述

弧玄武岩的成因: 进展与问题

徐义刚[1,2*], 王强[1,2,3], 唐功建[1,3], 王军[1], 李洪颜[1], 周金胜[1], 李奇维[1], 齐玥[1], 刘平平[4], 马林[1], 范晶晶[1]

1. 中国科学院广州地球化学研究所同位素地球化学国家重点实验室, 广州 510640;
2. 中国科学院大学地球与行星科学学院, 北京 100049;
3. 中国科学院青藏高原地球科学卓越创新中心, 北京 100101;
4. 北京大学地球与空间科学学院, 北京 100871
* 通讯作者, E-mail: yigangxu@gig.ac.cn

收稿日期: 2020-02-18; 收修改稿日期: 2020-08-31; 接受日期: 2020-09-03; 网络版发表日期: 2020-10-22
国家海洋局国际合作专项项目(编号: GASI-GEOGE-02)、国家自然科学基金重点项目(批准号: 91855215、41630208)和中国科学院战略性先导科技专项B类项目(编号: XDB18000000)资助

摘要 大洋俯冲带之上是否出现弧岩浆岩是汇聚板块边缘研究的前沿, 而与弧系统演化相关的最重要的岩石学问题是弧岩浆岩的起源. 作为弧岩浆体系中最重要的岩石类型, 弧玄武岩是揭示俯冲带地幔富集机制、壳-幔相互作用等深部动力学过程最重要的"岩石探针"之一. 俯冲大洋板片释放的流体或发生熔融产生的熔体在不同深度以不同比例交代地幔楔形成弧玄武岩的源区, 导致大部分弧玄武岩展示出富集大离子亲石元素和轻稀土元素、亏损高场强元素和重稀土元素的特征, 而小部分玄武岩则显示高Nb或富Nb特征. 还有少量在弧区分布的玄武岩表现出类似洋岛玄武岩或洋脊玄武岩的成分, 对其地幔源区是否受到俯冲组分影响还存在争议. 玄武质岩浆在上升过程中经历了分离结晶、岩浆混合乃至地壳混染等演化阶段, 直至最后喷出地表. 除了俯冲板片组分参与弧玄武岩地幔源区的形成外, 位于弧前的俯冲上盘物质也可能会通过板片拖曳作用或俯冲侵蚀作用进入弧下地幔加入到弧玄武岩源区. 此外, 弧下软流圈地幔角流带来的热和物质在弧玄武质岩浆的形成中也发挥了重要作用. 尽管近年来关于弧玄武岩的研究取得许多重要进展, 但弧下地幔交代作用及玄武岩源区的形成、弧玄武岩的产生与岩浆储库演化、弧玄武质岩浆作用与物质循环、产生弧玄武岩的动力学机制与板块构造的启动等领域尚需深入研究.

关键词 弧玄武岩, 岩石成因, 俯冲板片-地幔楔相互作用, 弧下地幔交代作用, 俯冲带

1 引言

大洋板块俯冲引起弧岩浆作用, 是现代板块构造理论的最重要成果之一(Frisch等, 2011). 但是, 在现今环太平洋俯冲带之上, 只有大约一半左右的地区有弧火山岩产出. 理解大洋俯冲带之上是否出现弧岩浆岩是汇聚板块边缘研究的前沿问题. 与弧系统演化相关的最重要的岩石学问题涉及玄武岩-安山岩-英安岩-流

中文引用格式: 徐义刚, 王强, 唐功建, 王军, 李洪颜, 周金胜, 李奇维, 齐玥, 刘平平, 马林, 范晶晶. 2020. 弧玄武岩的成因: 进展与问题. 中国科学: 地球科学, 50(12): 1818–1844, doi: 10.1360/SSTe-2020-0032
英文引用格式: Xu Y, Wang Q, Tang G, Wang J, Li H, Zhou J, Li Q, Qi Y, Liu P, Ma L, Fan J. 2020. The origin of arc basalts: New advances and remaining questions. Science China Earth Sciences, 63(12): 1969–1991, https://doi.org/10.1007/s11430-020-9675-y

© 2020 《中国科学》杂志社

纹岩组合的起源(Ringwood, 1974). 对于弧系统岩浆岩的研究最早可追溯到19世纪末期. 如在19世纪末, 与洋内弧密切相关的玻安岩(Boninite)已经被提出、命名和描述(Kikuchi, 1888, 1890). 20世纪早期已经对日本大陆边缘弧开展了火山岩岩石学的研究, Tomita(1935)在日本海周边发现新生代低硅富碱火山岩, 并将其命名为环日本海碱性岩省. 20世纪岩石学研究中一个最重要的进展, 就是揭示玄武岩是来源于地幔的部分熔融产物(Kushiro, 1959, 1968; Green和Ringwood, 1969). Kuno(1960)发现日本岛弧火山岩存在横向变化: 拉斑玄武岩出现在太平洋一侧, 而碱性玄武岩出现在日本海一侧, 认为前者形成于浅部地幔, 而后者来源于深部地幔. 自20世纪60年代起, 高温高压活塞-圆筒式装置实验技术被引入到地质研究领域, 极大地促进了对岛弧玄武岩岩石成因的研究. 后来的实验岩石学研究证实了Kuno模型(Yoder和Tilley, 1962, Kushiro, 1968). Tatsumi等(1983)通过反演计算日本大陆边缘弧原始玄武岩和实验岩石学研究, 提出拉斑玄武岩、高铝玄武岩和碱性玄武岩的形成深度分别为35、45~50和50~70km, 还发现玄武质岩浆形成的温度非常高(大于1300℃). 与此同时, 实验岩石学揭示了水在岛弧玄武岩成因中的重要作用: 水不仅可以降低地幔橄榄岩的固相线温度, 还可以改变熔体的成分(Kushiro, 1968; Grove等, 2012).

经过多年研究, 一个基本的共识就是弧玄武岩的形成与流体/熔体对弧下地幔楔的交代作用和热演化密不可分. 但是, 弧玄武岩形成机制仍然存在激烈的争论. 一些研究者提出, 弧玄武岩主要由俯冲洋壳释放的流体所交代的地幔楔熔融形成(Gill, 1981; Tatsumi等, 1986; Tatsumi, 1989; Hawkesworth等, 1993; Ulmer和Trommsdorff, 1995; Grove等, 2002). 而另外一些研究者则认为, 一些高Nb或富Nb的玄武岩是由俯冲洋壳产生熔体交代的地幔楔橄榄岩熔融而成(例如, Defant和Drummond, 1990; Defant和Kepezhinskas, 2001; Defant等, 2002). 弧玄武岩是弧岩浆系统中最重要的岩石类型之一, 记录了大洋俯冲带地幔富集机制和地幔深部动力学过程方面的重要的信息, 是探索地幔交代作用、物质循环以及深部动力学过程的重要“岩石探针”(Zheng等, 2020). 本文将重点综述新生代弧玄武岩成因研究的进展和存在问题, 并提出未来需要重点关注的研究方向.

2　弧的分类及相关的玄武岩特征、岩石组合

根据弧岩浆岩产出的位置, 一般将火山弧分为大洋弧(洋内弧)和大陆弧(图1). 洋内弧是由一个大洋岩石圈向另外一个大洋岩石圈之下俯冲所形成的, 其基底主要是硅镁质大洋地壳, 因此也被称为硅镁质岛弧(Frisch等, 2011). 新生代洋内弧主要分布于环太平洋地区北、西缘(图1), 包括阿留申、伊豆-小笠原-马里亚纳(IBM)、菲律宾-吕宋、班达、新不列颠-所罗门-新赫布里底(或瓦鲁阿图)、斐济-汤加-克马德克等群岛, 以及在大西洋西缘的小安德列斯和斯科舍弧等(Frisch等, 2011; 吴福元等, 2019). 不过近年来的研究发现, 大洋弧岩石圈可能包含有大陆碎块(例如, 吴福元等, 2019). 大陆弧是大洋岩石圈向大陆岩石圈之下俯冲所形成的, 其基底主要由大陆地壳(硅铝质物质)组成(Frisch等, 2011). 大陆弧主要包括北美、南美的西部以及印度洋东北缘的巽他弧(图1), 主要特点是其火山弧出现在大陆边缘且没有同大陆分离. 在大洋板块俯冲过程中, 如果上盘大陆板块出现弧后扩张导致原本位于大陆边缘的部分大陆岩石圈从大陆分离或出现在大陆架海域, 有时会构成新的俯冲带上盘. 在这些地区形成陆缘岛弧, 其中新生代陆缘岛弧主要分布在太平洋西北缘, 包括千岛群岛、日本-琉球等岛弧(图1).

弧玄武岩可以简单地分为拉斑(或低钾)、钙碱性、橄榄玄粗质(图2). 不同类型的玄武岩具有不同的岩石学、矿物学和地球化学特征. 同时, 洋内弧、大陆弧和陆缘岛弧系统玄武岩岩石组合、地球化学特征和成因也存在一定的差异.

2.1　洋内弧系统玄武岩及共生岩石组合

洋内弧系统岩石组合以玄武岩为主, 伴有少量安山岩-英安岩, 有时还有特殊的高镁安山岩类和埃达克岩(Kelemen等, 2003). 其中玄武岩以拉斑玄武岩和钙碱性玄武岩为主, 并有极少量的橄榄玄粗质玄武岩(例如, Hochstaedter等, 2000; Ishizuka等, 2003; Tatsumi等, 2008; Stern, 2010). 拉斑玄武岩主要出现在弧前和弧后盆地的位置, 如IBM洋内弧弧前火山岩组合主要为拉斑玄武岩(Ishizuka等, 2006, 2009; Reagan等, 2010). 这些拉斑玄武岩通常具有无斑隐晶结构, 极少斑晶结构;

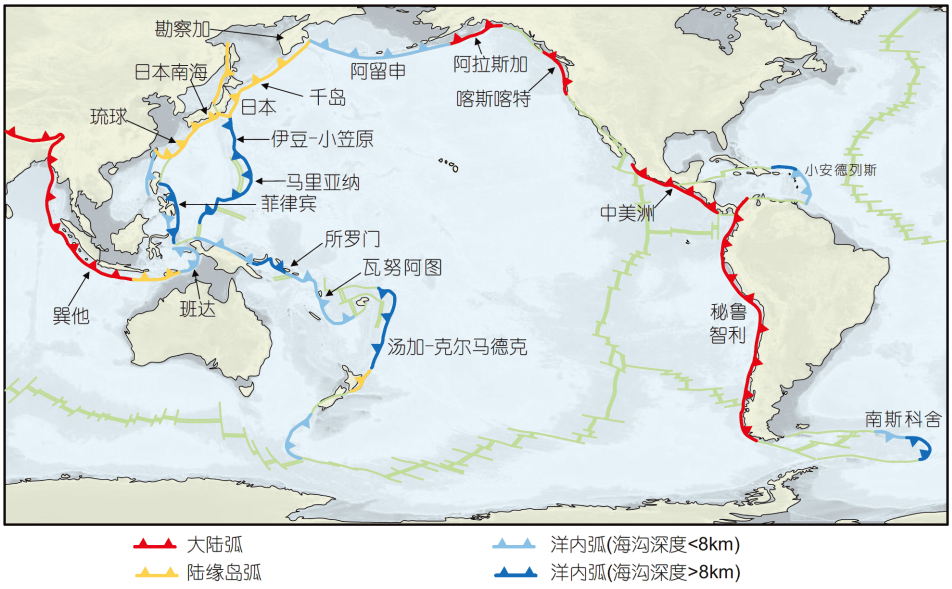


图 1　洋内弧、大陆弧和陆缘岛弧的分布

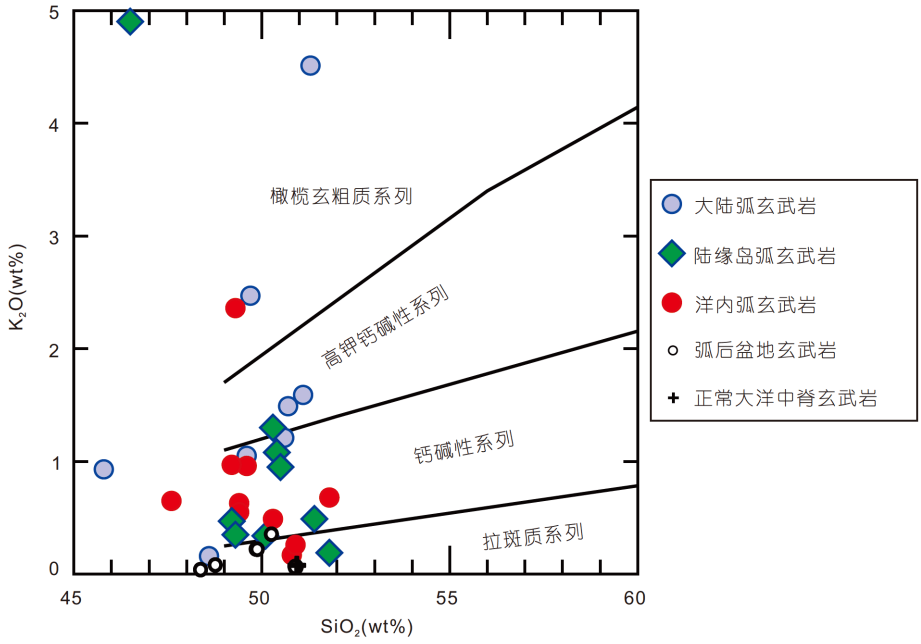


图 2　全球代表性洋内弧、大陆弧和陆缘岛弧原始玄武岩的硅-钾图

图中显示弧玄武岩主要分为拉斑和钙碱系列两种, 少量为橄榄玄粗质. 图中样品的数据都是经过筛选的、能够代表初始熔体的成分(Schmidt和Jagoutz, 2017)

主要矿物组成为橄榄石、斜长石和普通辉石, 有时含有少量斜方辉石和磁铁矿. 它们虽然富集大离子亲石元素(LILE)、亏损高场强元素(HFSE), 但是其轻重稀土元素分异不显著, 轻稀土(LREE)富集不明显, 因此并不具有典型的岛弧玄武岩特征. 在微量元素蛛网图上, 除了Nb-Ta亏损和LILE富集外, 整体上呈相对平滑的分布特征(图3a和3b). 一般将洋内弧拉斑玄武岩成因归咎于俯冲大洋板片脱水形成的富水流体向上运移引发地幔楔水化并熔融而成(Kelemen等, 2003; Reagan等, 2010).

钙碱性玄武岩往往出现在成熟的洋内弧中，如瓦努阿图、所罗门等(Peate等, 1997; Schuth等, 2009; Beaumais等, 2016). 钙碱性玄武岩有时因高Al_2O_3含量而被称为高铝玄武岩(Stern, 2010). 钙碱性玄武岩基本为斑状结构，其斑晶为斜长石、橄榄石、普通辉石和磁铁矿，偶尔出现角闪石. 虽然具有与拉斑玄武岩相似的地球化学特征(图3a和3b)，但它更加富集LILE和LREE，而且两者含量的变化范围更大(图3a和3b). 与洋中脊玄武岩(MORB)相比，大多数洋内弧钙碱性玄武岩往往具有略微富集的Nd-Hf同位素组成，与其源区有大洋俯冲沉积物的加入有关(Beaumais等, 2016). 但是，目前普遍认为洋内弧中拉斑玄武岩和钙碱性玄武岩具有相似的成因机制，只是其地幔楔亏损程度和俯冲板片组分加入的程度不同而已(Schmidt和Jagoutz, 2017).

橄榄玄粗质玄武岩在洋内弧中很少出现，只见于斐济、巴布新几内亚和菲律宾弧等地，且主要出现在远离海沟的位置(如后弧区(Rear-arc))(Müller等, 2001; Scherbarth和Spry, 2006; Leslie等, 2009; Wolfe和Cooke, 2011). 橄榄玄粗质玄武岩斑晶主要为橄榄石和普通辉石, 以及少量的角闪石、磁铁矿和斜长石. 与钙碱性玄武岩和拉斑玄武岩相比，橄榄玄粗质玄武岩强烈富集LREE和LILE，并显示显著的轻重稀土分馏(Leslie等, 2009). 因此，橄榄玄粗质玄武岩是经俯冲大洋沉积物交代的富集岩石地幔通过低程度部分熔融而成(Leslie等, 2009).

2.2　大陆弧系统玄武岩及共生岩石组合

大陆岩石圈由于其低密度、高浮力的特征，通常作为俯冲带的上盘，其俯冲带(如南美洲的安第斯-科迪勒拉造山带)几何结构与洋内弧非常相近. 由于大陆地壳物质加入到俯冲带系统以及较厚的陆壳和大陆岩石圈，大陆弧玄武岩在成因和成分上与洋内弧玄武岩略有差异. 大陆弧产出大量安山质岩浆岩，伴有英安岩和流纹岩等，玄武岩以钙碱性为主，不同于洋内弧玄武岩的多样性(拉斑、低钾、高钾钙碱性和橄榄玄粗质)(Wilson, 1989; Winter, 2014). 已发现的大陆弧拉斑玄武岩主要出现在北美西部喀斯喀特(Cascades)火山弧(Schmidt和Jagoutz, 2017; Mullen等, 2017), 且主要为高铝拉斑玄武岩(Mullen等, 2017). 高铝橄榄石拉斑玄武岩的主量元素、微量元素丰度与MORB相似(图3e~3f)，但具有更高的Al_2O_3(>17.0wt%)、CaO和更低的SiO_2、H_2O(<0.2wt%)含量(Bacon等, 1997; Le Voyer等, 2010; Sisson和Layne, 1993). 这套拉斑质岩石可能是含水尖晶石橄榄岩地幔经低程度(6~10%)部分熔融而成(Baker等, 1994). 钙碱性玄武岩普遍出现于全球各主要的大陆弧，尤以美洲西部的安第斯弧和科迪勒拉造山带最为典型. 在地球化学组成上，大陆弧拉斑玄武岩有比MORB高的不相容元素丰度，但亏损HFSE(图3e~3f). 相对于洋内弧玄武岩，大陆弧玄武岩显示高的K/Rb和Fe/Mg比值，以及更为宽广的$^{87}Sr/^{86}Sr$、$^{143}Nd/^{144}Nd$和Pb同位素组成，这可能与聚集于海沟附近的陆源沉积物随俯冲加入大陆弧岩浆源区有关(Winter, 2014; Zheng等, 2020). 大陆弧产出的橄榄玄粗质岩石一般也出现在远离海沟的位置，由近到远同拉斑序列和钙碱性序列一起构成带状分布(Morrison, 1980; Bloomer等, 1989; Lin等, 1989). 在时间上, 安第斯山地区的橄榄玄粗质岩石为最年轻的岩浆序列，出现在拉斑系列和钙碱性系列之后(Müller等, 1992; Scherbarth和Spry, 2006; Beccaluva等, 2013). 有研究观察到，在火山弧的同一位置钙碱性岩石和橄榄玄武粗质玄武岩岩石伴生，被解释为俯冲板片突然变陡所致(Morrison, 1980; Beccaluva等, 2013).

2.3　陆缘岛弧系统玄武岩及共生岩石组合

陆缘岛弧虽然已经是大陆岩石圈的一部分，但是其陆壳厚度有限. 陆缘岛弧火山岩以玄武岩-安山岩等为主, 其中玄武岩主要以钙碱性为主, 并有少量的拉斑质和橄榄玄武粗质(Tatsumi等, 2008; Shuto等, 2015; Lai等, 2017). 另外，陆缘岛弧也出现一些特殊的岩石组合, 包括与洋岛玄武岩(OIB)成分相似的洋岛型玄武岩、富Nb玄武岩、赞岐岩和埃达克岩等(Kimura和Ariskin, 2014; Hanyu等, 2002; Tatsumi, 2006). 拉斑玄武岩虽然主要出现在不成熟的洋内弧，比如马里亚纳、汤加洋内弧等(Ishizuka等, 2003; Meffre等, 2012), 但在一些陆缘岛弧如日本岛弧、千岛群岛岛弧等也有出现(Shuto等, 2015; Kuritani等, 2008).

在一些岛弧，穿岛弧地球化学的不均一性是陆缘岛弧玄武岩的一个显著特征，其中弧前玄武岩主要由拉斑玄武岩和少量钙碱性玄武岩组成，而弧后玄武岩主要为钙碱性玄武岩和少量碱性玄武岩(Tatsumi等,

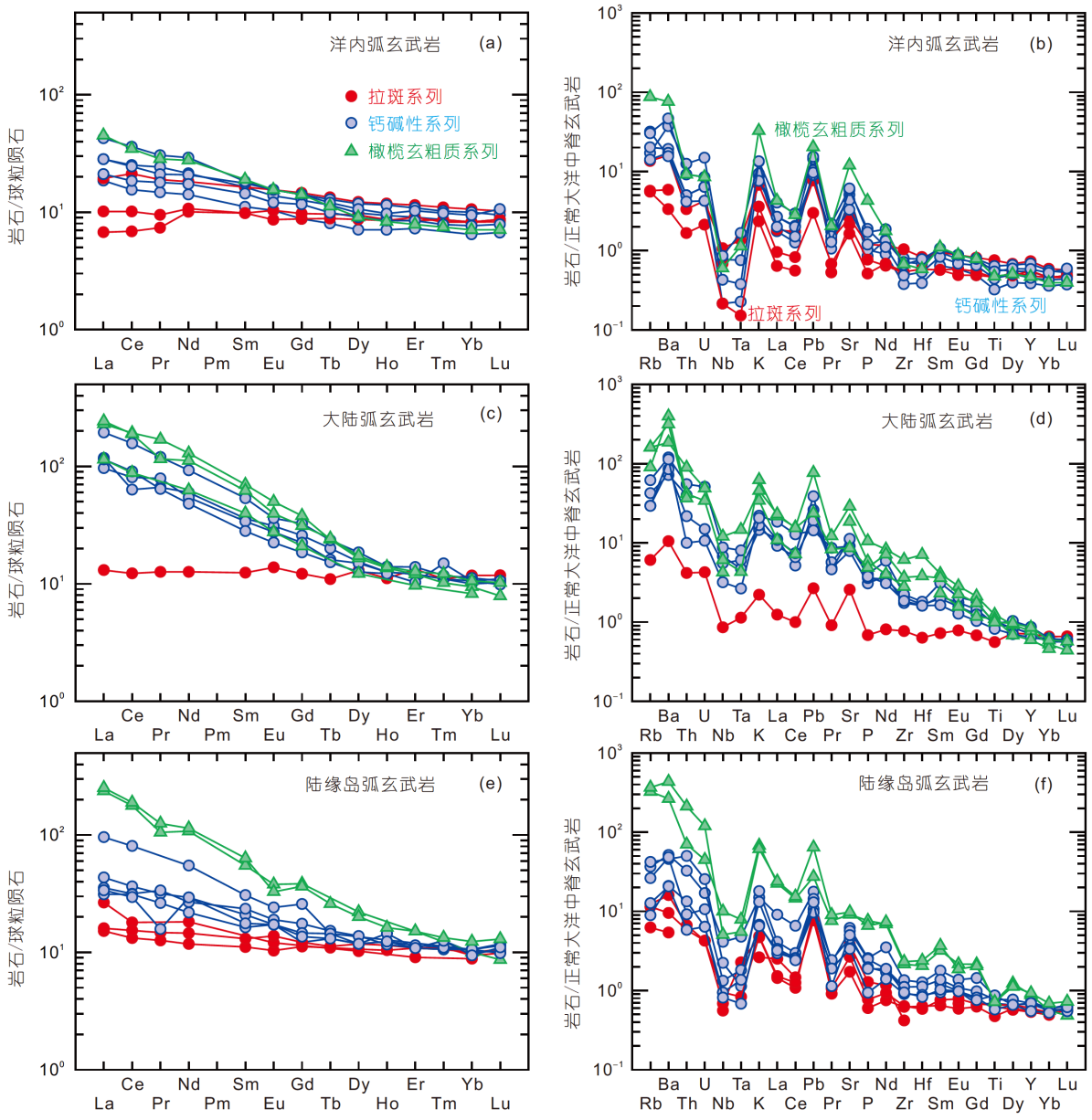


图 3　全球代表性洋内弧、大陆弧和陆缘岛弧和原始玄武岩的稀土和微量元素分配图

数据来源于Schmidt和Jagoutz(2017): 洋内弧包括俾斯麦群岛、斐济、伊豆-小笠原、马里亚纳、克尔马德克、小安的列斯、帕劳、所罗门和瓦努阿图; 大陆弧包括安第斯、中美洲、墨西哥、喀斯喀特和巽他弧等; 陆缘岛弧包括日本、千岛、勘察加和新西兰等. 球粒陨石和正常大洋中脊玄武岩. 标准化数值引自Sun和McDonough(1989)

2008). 拉斑玄武岩的主要组成矿物为橄榄石、斜长石、普通辉石和斜方辉石. 拉斑玄武岩虽然具有典型的岛弧岩浆特征(图3c和3d), 但其轻重稀土元素分异不明显, 亏损Nb-Ta而富集Sr-Pb, 整体上显示平滑的微量元素蛛网图特征(图3c和3d). 与洋内弧拉斑玄武岩相比, 陆缘岛弧拉斑玄武岩稍微富集LILE和LREE(图3c和3d). 陆缘岛弧钙碱性玄武岩主要出现在弧后的位置, 如日本东北岛弧中的弧后地区(Shuto等, 2015). 陆缘岛弧中钙碱性玄武岩与洋内弧中的钙碱性玄武岩相似, 但是前者往往更加富集LREE和LILE(图3c和3d), 后者比前弧拉斑玄武岩具有更高的HFSE(如Nb和Zr)含量和更高的稀土元素含量.

对于陆缘岛弧中弧前和弧后玄武岩地球化学成分的差异有多种解释. 目前普遍认为这种差异与大洋俯冲组分的改变无关, 更可能与弧下地幔的部分熔融程度有关. 弧前和弧后玄武岩的地幔源区均受到俯冲沉积物的影响, 但弧前玄武岩形成于浅部(30~50km)软流圈地幔的高程度部分熔融, 而弧后玄武岩来源于深部(60~75km)软流圈地幔的低程度部分熔融(Shuto等, 2015). 在陆缘岛弧(如千岛群岛)中, 偶尔出现一些橄榄玄粗质岩石, 其斑晶主要为普通辉石、斜方辉石、角闪石、金云母和长石等. 这些橄榄玄粗质岩石主要由富集的岩石圈地幔熔融所形成(Elburg和Foden, 1999).

洋内弧、大陆弧和陆缘岛弧系统的玄武质岩石在Sr-Nd同位素组成上显示出系统性差别(图4): 洋内弧玄武质岩石基本显示亏损的Sr-Nd同位素特征(图4a), 大陆弧拉斑和钙碱性玄武质岩石总体显示略微亏损的Sr-Nd同位素组成, 但橄榄玄粗质岩石则显示富集Sr-Nd同位素组成(图4c); 陆缘岛弧玄武质岩石总体上显示亏损的Sr-Nd同位素特征, 但部分样品在向富集组分方向演化(图4b). 从洋内弧、陆缘岛弧到大陆弧, 其玄武质岩石的Sr-Nd同位素组成逐渐富集, 变化范围逐渐变大. 同洋内弧、陆缘岛弧中的橄榄玄粗质岩石相比, 大陆弧橄榄玄粗质岩石具有明显富集的Sr-Nd同位素组成(图4), 这很可能与后者源区为古老的岩石圈地幔或包含更多的沉积物组分有关(例如, Carlier等, 2005; Winter, 2014).

陆缘岛弧系统和大陆弧系统存在一定的差异: 前者(如日本、千岛弧)存在弧后拉张, 岩浆产物为玄武岩-安山岩; 后者(如安第斯弧)缺乏弧后拉张, 产物以安山岩为主(Frisch等, 2011). 造成上述差别的原因可能与俯冲板片的年龄、俯冲角度以及俯冲的深部动力学过程等因素有关(Winter, 2014; Frisch等, 2011; 王强等, 2020). 以新生代环太平洋弧为例, 太平洋西侧板片的俯冲由于板片老、密度相对大以高角度俯冲为主, 且俯冲板片发生了回卷, 引发了大规模软流圈上涌和弧后拉张, 形成了弧后盆地, 并导致日本、千岛陆缘弧地区玄武岩-安山岩组合的形成. 与此相比, 太平洋东侧的俯冲由于板片年轻、密度相对小以相对低角度的俯冲为主, 导致软流圈地慢楔很小或不明显, 且俯冲上盘以挤压构造背景为主, 没有形成弧后盆地, 但地壳明显增厚, 产生的岩浆以板片熔融、混杂岩熔融或来自地幔岩浆在中下地壳发生了经历了复杂的演化, 典型的如熔融、同化混染、存储和均一(MASH)过程, 最后形成安第斯大陆弧地区以安山岩为主的弧岩浆岩. 但是就俯冲板片倾角随时间的演化来说, 也有研究

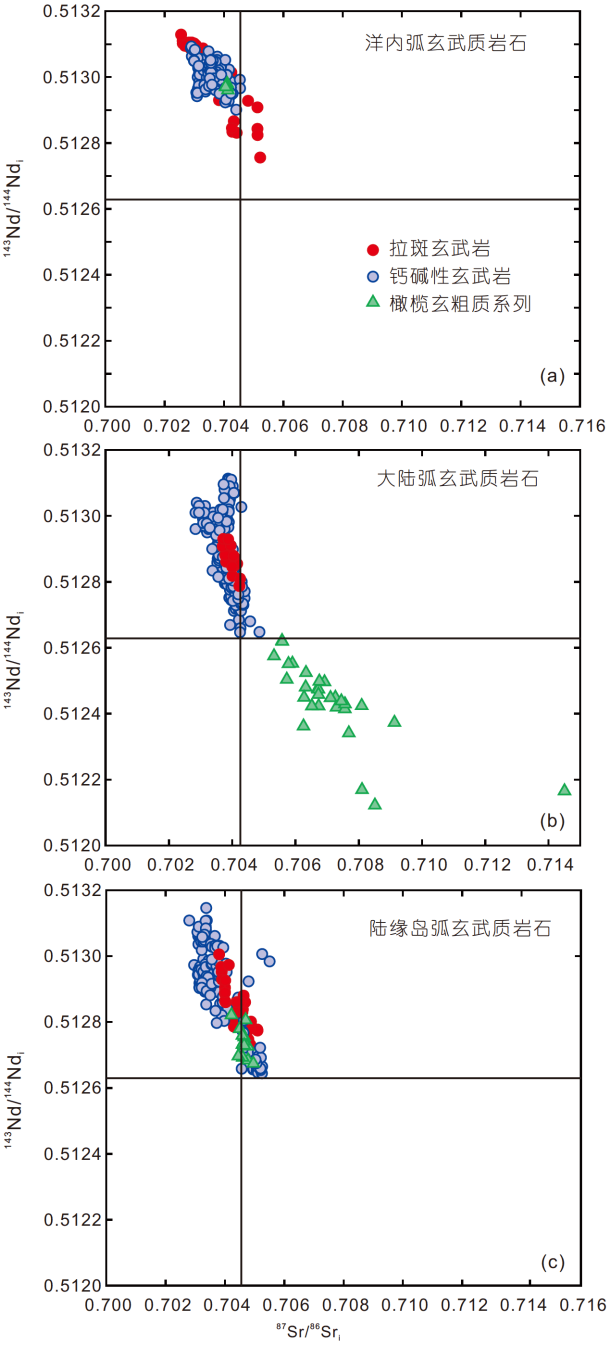


图 4　全球代表性洋内弧、大陆弧和陆缘岛弧玄武岩Sr-Nd同位素图解

洋内弧、陆缘弧和大陆弧数据与图3一致. 数据来源于georoc数据库(http://georoc.mpch-mainz.gwdg.de/georoc/)

认为西太平洋俯冲板片倾角经历了由缓到陡的两阶段过程，而东太平洋俯冲板片倾角经历了由缓到陡再到缓的三阶段过程.

3 特殊类型的弧系统玄武质岩石

3.1 高Nb或富Nb玄武岩

高Nb岛弧玄武岩的概念最早由Defant等(1991, 1992)在研究东太平洋新生代弧玄武岩时提出来. 他们在北美巴哈加利福利亚(Baja California)、墨西哥、南华盛顿喀斯喀特(Southern Washington Cascades)、巴拿马拉耶瓜达(La Yeguada)和拉丁美洲巴拿马大陆弧地区发现了粗面玄武岩-橄榄玄粗岩. 这些岩石具有高Nb量(>20ppm, 1ppm=1μg g^{-1})或Nb亏损不明显的特征(图5)(Defant等, 1991, 1992), 不同于"正常的弧玄武岩"通常显示的低Nb含量或Nb-Ta-Ti的强烈亏损特征(图3). Sajona等(1993, 1994, 1996)提出的"富Nb岛弧玄武岩"是指岛弧中具有富集的Nb(Nb=7~16ppm, Na/La>0.5)或Nb亏损不明显的玄武岩(图5), 主要出现在西太平洋菲律宾三宝颜半岛(Zamboanga peninsula)和棉兰老岛(Mindanao), 以及东太平洋南美厄瓜多尔大陆弧(图5)(Beate等, 2001; Bourdon等, 2003). 无论是高Nb还是富Nb玄武岩, 常与高镁安山岩-埃达克岩共生出现, 被认为是由俯冲板片熔融产生的埃达克质熔体交代地幔楔橄榄岩熔融而成(例如, Sajona等, 1993, 1996; Defant和Kepezhinskas, 2001; Defant等, 2002; Wang等, 2007).

3.2 洋岛型玄武岩

洋岛型玄武岩具有与洋岛玄武岩相似的微量元素特征, 一方面与弧玄武岩一样富集LILE, 轻重稀土分异明显, 另一方面没有明显的Nb-Ta亏损(图5). 这类玄武岩主要出现在以下特殊的俯冲环境: (1) 地幔柱影响的弧环境, 比如汤加(Tonga)弧北端(Falloon等, 2007; Price等, 2014), 即相邻的Samoa地幔柱向西流入Tonga弧后区域, 形成具有高$^3He/^4He$的OIB型玄武岩; (2) 板片窗(活动的洋脊俯冲)环境, 比如北科迪勒拉(Northern Cordilleran)弧(Mullen和Weis, 2013; Thorkelson等, 2011), 即俯冲大洋板片之下的热软流圈地幔通过板片窗上涌至弧下地幔楔, 发生降压熔融; (3) 异常热的俯冲带, 如Cascades弧(Leeman等, 2005; Carlson等, 2018), 即年轻的、热的Juan de Fuca大洋板片在弧前区域已经完全脱水, 所以弧下地幔楔受俯冲组分影响较小. 上述新生代俯冲带洋岛型玄武岩的地幔源区都缺少板片来源的富水溶液, 但是富含俯冲板片来源的含水熔体. 在地幔楔熔融机制上, 一般认为是相对干的、热的地幔上涌导致的减压熔融, 类似于洋中脊或地幔柱, 因此不会出现典型弧玄武岩中亏损HFSE特征. 但是, Zheng(2019)对这个解释提出异议, 认为俯冲板片在>1200℃条件下熔融时其中的金红石会发生分解, 所产生的板片熔体就显著出富集HFSE的特点, 由此交代地幔楔橄榄岩就形成了洋岛型玄武岩的地幔源区.

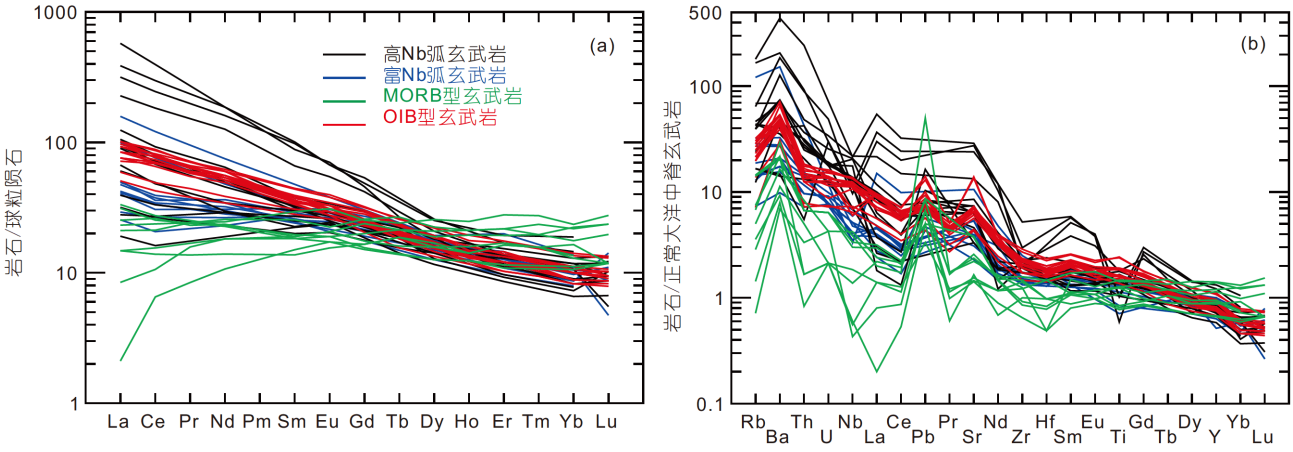


图 5 全球特殊弧玄武质岩石的稀土和微量元素分配图

数据来源: 高/富Nb弧玄武岩(Bourdon等, 2003; Castillo等, 2007; Defant等, 1992; Kepezhinskas和Defant, 1996; Sajona等, 1996); OIB型弧玄武岩(Mullen和Weis, 2013); MORB型弧玄武岩(Cole和Stewart, 2009; Sorbadere等, 2013b); 标准化数值根据Sun和McDonough(1989)

由于洋岛型玄武岩所产出的俯冲带往往存在热的深部地幔上涌, 地球物理、地球化学以及实验模拟表明, 这些俯冲带地区可能存在深源的地幔柱. 但这些观点仍存在许多争议, 如Cascades弧火山和High Lava Plains火山链的关系以及与黄石地幔柱是否存在关联等(Liu和Stegman, 2012; Kincaid等, 2013). 还有研究发现, 一些高Nb或富Nb弧玄武岩没有明显的Nb负异常甚至显示正Nb异常, 类似于洋岛玄武岩, 其形成被解释为地幔楔中富集组分的熔融(Castillo等, 2002)、洋脊俯冲造成的板片窗大洋软流圈地幔上涌发生熔融(Gorring等, 2003; Thorkelson等, 2011; Tang等, 2010)以及俯冲洋壳熔体(金红石发生了分解)交代的地幔深部源区熔融(Ringwood, 1990; Zheng等, 2020).

3.3 E-MORB型玄武岩

有些弧前位置也产出与MORB微量元素特征相似的MORB型玄武岩, 如在IBM岛弧的弧前(DeBari等, 1999; Reagan等, 2010; Ishizuka等, 2011; Shervais等, 2019)和中美洲火山岛弧的弧前位置(Whattam, 2018). 此外, MORB型玄武岩偶尔也出现在岛弧环境中与岛弧玄武岩共生(如在瓦努阿图岛弧; Sorbadere等, 2013b). 像MORB一样, 这些MORB型玄武岩也具有正常与富集之分, 分别类似与N-MORB和E-MORB. 其中E-MORB型玄武岩未显示HFSE亏损, Nb的含量与富Nb玄武岩相似(图5). E-MORB型玄武岩源区受到少量(~0.2wt%)俯冲板片流体的交代(Sorbadere等, 2013a). 另外一些洋脊俯冲下岛弧中也产出E-MORB型玄武岩, 比如在阿拉斯加和美国西部的洋脊俯冲(Cole和Stewart, 2009). 阿拉斯加玄武岩具有N-MORB型玄武岩特征, 而美国西部洋脊俯冲成因的玄武岩具有E-MORB型玄武岩的特征. 两类玄武岩均具有亏损地幔的Sr-Nd同位素特征(Cole和Stewart, 2009). 这些俯冲带的MORB型玄武岩都与上覆薄的弧地壳强烈伸展有关, 比如地壳规模的深大断裂、洋脊俯冲和初始俯冲诱发的伸展, 代表了上涌的地幔发生降压熔融形成的产物.

3.4 高铝玄武岩

早期研究发现, 俯冲带存在大量Al_2O_3含量大于16wt%的高铝玄武岩, 其MgO含量通常小于7wt%, 含有更多钙长石而区别于拉斑玄武岩(Kuno, 1960; Hamilton, 1964; Crawford等, 1987). 原先认为这些高铝玄武岩是俯冲的榴辉岩板片高程度熔融的产物(Brophy和Marsh, 1986), 但后来这种观点逐渐被摒弃(Brophy, 1989). 现在普遍认为, 高铝玄武岩是富水(>2wt%)的原始弧玄武质岩浆在长石结晶受到抑制后的分异产物(Beard和Lofgren, 1992; Blatter等, 2013; Melekhova等, 2015; Pichavant和MacDonald, 2007; Sisson和Grove, 1993; Xie等, 2016), 即主要分异结晶橄榄石和单斜辉石. Parman等(2011)统计了不同含水量的岩浆的分异结晶实验结果, 发现分异的岩浆所能达到的最高Al_2O_3含量与岩浆水含量成正比, 即岩浆水含量越高, 长石结晶受到抑制程度越强, 分异岩浆的峰值Al_2O_3含量越高. Pichavant和MacDonald(2007)统计了斜长石饱和的含水玄武质熔体的Al_2O_3含量(<4kbar实验数据), 发现其与岩浆的水含量成正相关关系. 此外, 不同压力(0.4~0.9GPa)条件下含水玄武质岩浆的结晶实验表明, 高压条件抑制了斜长石的结晶, 这更有利于形成低镁的、演化的高铝玄武岩(Blatter等, 2013; Xie等, 2016).

4 弧玄武岩的成因

弧玄武岩的成因涉及源区特征、部分熔融、结晶分异等过程.

4.1 弧下地幔楔交代作用与玄武岩源区的形成

4.1.1 俯冲板片脱水与流体交代作用

典型的弧玄武岩富集LILE(如Cs、Rb、K、Ba、Pb和Sr)和LREE、亏损HFSE(如Ta、Nb、Zr和Ti)和重稀土元素(HREE)(图3). 这些微量元素地球化学特征是弧玄武岩地幔源区受到俯冲带流体交代的典型特征(例如, Tatsumi等, 1986; Tatsumi, 2005; Zheng, 2019). 俯冲大洋板片由沉积岩、玄武岩、辉长岩和橄榄岩组成, 其中有许多富水矿物, 如云母类(多硅白云母、黑云母、钠云母等)、闪石类(锰闪石、蓝闪石、冻蓝闪石、韭闪石)、硬柱石、黝帘石、绿帘石、硬绿泥石、绿泥石、滑石和蛇纹石等, 它们的含水量为2.0~18.0wt%不等. 这些矿物俯冲到不同深度(30~250km范围, 甚至大于250km)会发生脱水作用, 产生的流体对上覆的地幔楔进行交代, 形成玄武岩的源区(Tatsumi等, 1986; Brenan等, 1995; Keppler, 1996; Schmidt和Poli, 2014; 郑永飞等, 2016).

在一些新生代大陆弧(如北美西部雷尼尔峰地区)

发现了俯冲板片释放的流体进入地幔楔并触发弧岩浆作用的地球物理证据(McGary等, 2014). 含水流体和榴辉岩组合矿物(石榴石、单斜辉石和金红石)在900~1200℃和3.0~5.7GPa条件下的分配实验表明, 石榴石和纯的辉石不能导致HFSE与LILE间的明显分异, 但含1.5%金红石榴辉岩释放的流体, 可以导致HFSE与LILE的分异, 并导致地幔楔选择性富集LILE而亏损HFSE(Stalder等, 1998; Foley等, 2000). 新近兴起的非传统稳定同位素研究为上述观点提供了支持证据. 例如, 一些洋内弧(如中美洲的小安德列斯弧)玄武岩具有重的Mg同位素组成, 可能与俯冲板片释放流体的交代作用有关(图6a)(Teng等, 2016). 弧玄武岩具有较大的Li同位素组成范围(δ^7Li=−8.4~11.4‰)(Su等, 2016). 其中大部分与MORB类似, 但中美洲大陆弧和Lesser Antilles、IBM等洋内弧玄武岩的Li同位素组成不同于MORB, 与受俯冲板片物质(流体/熔体)的交代、板片脱水及水-岩相互作用等过程有关(Moriguti和Nakamura, 1998; Chan等, 2002; Agostini等, 2008; Bouvier等, 2008, 2010; Tang等, 2014).

新生代弧玄武岩具有较大的B同位素变化范围(δ^{11}B=−9~+16‰)(De Hoog和Savov, 2017). 板片俯冲过程中B同位素分馏遵循瑞利分馏过程, 板片脱流体时大量的重B同位素(^{11}B)倾向于富集在流体中, 导致俯冲板片中B含量下降且B同位素组成逐渐变轻(图6b)(De Hoog和Savov, 2017). 越来越多的研究认为, 弧火山岩高的δ^{11}B不仅与板片流体/熔体的交代有关, 还可能受到了弧前流体改造的蛇纹石化地幔或混杂岩的影响(Benton等, 2004; Savov等, 2005, 2007; Pabst等, 2011; Tonarini等, 2011; Scambelluri和Tonarini, 2012; Spandler和Pirard, 2013; Konrad-Schmolke等, 2016; Martin等, 2016; Zhang等, 2017; Prigent等, 2018).

传统的观点认为, 俯冲大洋板片释放的流体交代地幔楔是导致弧岩浆岩源区形成的重要机制, 且随着大洋板片俯冲深度增加, 板片释放的流体逐渐减少(例如, Ishikawa和Nakamura, 1994). 但对西太平洋马里亚纳弧前地质研究表明, 俯冲板片在弧前(蓝片岩相条件)已丢失了5.5wt%的H_2O(Schmidt和Poli, 1998), 且13%的弧前地幔会在20~60km的深度被蛇纹岩化(Savov等, 2007). 这些浅部蛇纹岩化地幔可通过拖曳-俯冲或俯冲侵蚀作用进入地幔深部, 参与幔源岩浆的形成.

4.1.2 俯冲板片熔融与熔体交代作用

俯冲板片除了释放流体外, 在一些特殊条件下(如年轻的、热的洋壳), 还会发生熔融, 产生埃达克质熔体(Defant和Drummond, 1990; Peacock等, 1994). Nicholls和Ringwood(1973)最早提出俯冲板片发生熔融形成的熔体交代地幔楔. Elliott等(1997)提出俯冲板片熔体会同流体一样改变或交代地幔楔橄榄岩, 使其成为弧玄武岩的潜在源区. 实验岩石学和弧下地幔橄榄岩包体的研究表明, 板片熔体比含水流体具有更强的携带高场强元素的能力(例如, Kepezhinskas等, 1995, 1997; Keppler, 1996; Defant和Kepezhinskas, 2001), 而且这些熔体会同地幔反应形成富角闪石、金云母和高场强元素的地幔源区(Kepezhinskas等, 1997; Wang等, 2008). 另外一种可能性是俯冲板片在深部金红石不稳定区发生熔融, 产生的熔体交代了深部地幔源区(例如, Ringwood, 1990; Zheng, 2019).

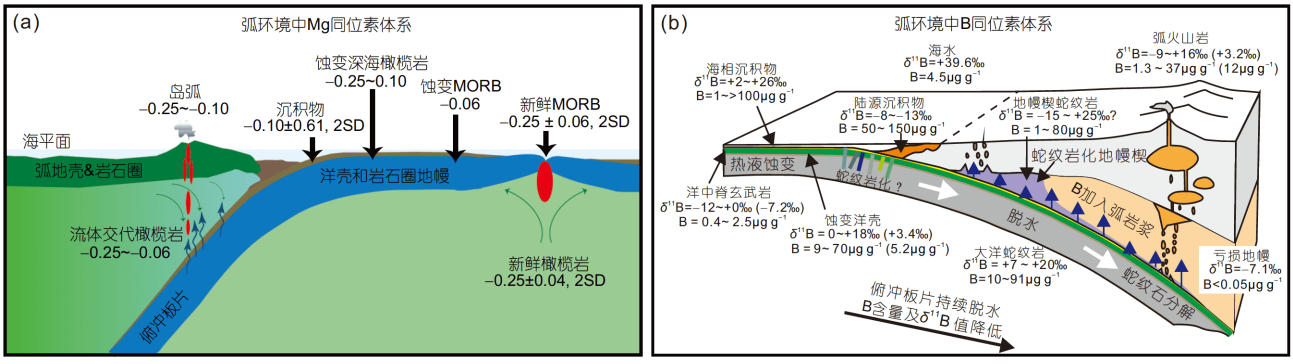


图 6　洋内弧和大陆弧玄武岩的Mg(a)和B(b)同位素演化示意图

据Teng等(2016)、De Hoog和Savov(2017)

事实上, 一些新生代弧(如菲律宾、巴拿马、墨西哥巴哈半岛、勘察加等)出现了只有在板内环境中才可能出现的富Nb或高Nb玄武岩, 被认为其源区受到了板片熔体的交代(例如, Sajona等, 1996; Defant和Kepezhinskas, 2001; Aguillón-Robles等, 2001). 这些地区产出富Nb或高Nb玄武岩-高镁安山岩-埃达克岩的组合(例如, Sajona等, 1996; Defant和Kepezhinskas, 2001; Defant等, 2002; Wang等, 2007), 不同于由俯冲流体交代地幔楔橄榄岩熔融产生的玄武岩-安山岩-英安岩-流纹岩组合. Mo同位素组成可以有效识别不同类型俯冲板片物质的贡献. 板片流体交代地幔楔形成的熔岩具有高的δ^{98}Mo值(−0.1~+0.24‰), 而板片熔体交代地幔楔形成的熔岩具有低的δ^{98}Mo值(−0.72~−0.1‰)(Freymuth等, 2015; König等, 2016). 受俯冲还原性沉积物(如黑色页岩)熔体交代地幔楔形成的熔岩具有高的δ^{98}Mo(+0.02~+0.34‰), 而受氧化性沉积物交代地幔楔形成的熔岩具有相对低的δ^{98}Mo(−0.88~−0.06‰)(Freymuth等, 2016; Gaschnig等, 2017).

俯冲洋壳在弧下深度的部分熔融及后续的熔体-橄榄岩反应可能是岛弧系统中一个非常普遍的过程(例如, Spandler和Pirard, 2013; Kelemen等, 2014; Schmidt和Jagoutz, 2017; Zheng等, 2020). 蛇绿岩和地幔捕虏体的岩石学研究表明, 俯冲带中存在多种类型的熔体与地幔楔橄榄岩反应(Ertan和Leeman, 1996; Varfalvy等, 1996; McInnes等, 2001; Tamura和Arai, 2006; Bénard和Ionov, 2013). 当洋壳俯冲到弧下地幔时会发生部分熔融形成长英质熔体(Rapp和Watson, 1995; Rapp等, 1999; Hermann和Spandler, 2008; Spandler等, 2010; Duncan和Dasgupta, 2014; Schmidt, 2015; Sisson和Kelemen, 2018), 这些熔体从俯冲板片中抽提后, 在浮力的作用下向上迁移, 并交代周围的地幔楔橄榄岩. 此外, 受交代的地幔橄榄岩发生部分熔融会形成镁铁质岩浆, 后者在上升过程中也会进一步与地幔橄榄岩发生反应(Van den Bleeken等, 2010, 2011; Lambart等, 2012; Wang等, 2013, 2016).

4.1.3　板片流体/熔体进入弧玄武岩地幔源区的方式

板片来源的俯冲组分进入弧玄武岩地幔源区的方式主要有三种(见Spandler和Pirard, 2013及其中的参考文献): (1) 沿着地幔矿物颗粒边界形成的渗透流(porous flow); (2) 沿着地幔裂缝形成的通道/集中流(focussed flow); (3) 俯冲隧道内的固体混杂岩形成的底劈流(diapiric flow). 俯冲组分以上述不同方式上升的速率不一样, 且在上升过程中成分变化程度和对地幔橄榄岩的改造程度也不一样. 值得注意的是, 渗透流过程会形成大量的含水交代矿物, 导致残余流体的微量元素特征显著偏离弧玄武岩, 因此经过渗透反应之后的流体不是玄武岩源区的主要组分(Pirard和Hermann, 2015), 但之前形成的地幔交代岩可以成为玄武岩源区.

4.2　弧下地幔部分熔融与热结构

导致地幔发生部分熔融有三个机制, 即减压、加水和升温(徐义刚, 1999; Niu, 2005). 对全球岛弧岩浆斑晶的熔融包裹体测定发现, 岛弧岩浆中的水含量在2~6wt%, 平均为(3.9±0.4)wt%(Plank等, 2013), 远高于洋中脊玄武岩的含水量. 实验岩石学研究表明, 水的加入会大大降低橄榄岩的熔融温度, 含水的地幔橄榄岩在高压下(>2.5GPa)或者低压高比例(>25%)部分熔融会产生玄武质岩浆(Green, 1973; Gaetani和Grove, 1998; Irving和Green, 2008; Tenner等, 2012; Green等, 2014), 因此加水是诱导弧下地幔发生部分熔融的主要因素.

目前不同实验得到的橄榄岩湿固相线温度差别很大, 在3GPa压力条件下, 橄榄岩湿固相线可低至~800℃(Grove等, 2006; Till等, 2012), 或高达1000~1100℃(Green等, 2010, 2012), 这种固相线温度的巨大差异会影响关于岛弧玄武质岩浆成因机制的认识. 如果湿固相线低至~800℃, 那么意味着地幔楔底部就可以发生绿泥石化橄榄岩的脱水熔融或水饱和橄榄岩熔融(Grove等, 2009; Till等, 2012), 即板片释放的水进入弧前地幔和底部地幔楔可以形成绿泥石化橄榄岩, 而绿泥石脱水线与水饱和橄榄岩固相线的重叠区域即为弧岩浆生成的温压范围. 但如果湿固相线高达1000~1100℃, 那么俯冲板片之上的地幔楔橄榄岩并不会因为加水而立即发生熔融. 大部分研究者认为, 板片来源的俯冲组分(流体/熔体)需要穿越地幔楔底部的湿固相线以下的橄榄岩, 然后再进入到地幔楔核部高温区域中玄武岩源区(Spandler和Pirard, 2013; Pirard和Hermann, 2015; Prigent等, 2018); 或者俯冲组分先交代地幔楔底部橄榄岩形成交代岩, 然后这些地幔交代

岩部分熔融形成玄武岩(Manning, 2004; Grove等, 2009; 郑永飞等, 2016). 因此岛弧岩浆的形成, 不仅受控于俯冲板块的脱水作用, 还与俯冲带热结构和热演化密切相关(Zheng, 2019). 水化橄榄岩受到后期加热就会熔融, 加热机制主要是俯冲板片与地幔楔的解耦和软流圈地幔侧向填充效应(Manning, 2004; 郑永飞等, 2016). 这种交代的水化橄榄岩甚至可以在大洋俯冲阶段不发生熔融, 而储存在岩石圈地幔中, 在陆陆碰撞后的伸展阶段发生熔融(Xu等, 2004; 郑永飞等, 2015).

板块的起始俯冲过程会形成一些特殊的岩石类型, 比如弧前玄武岩和玻安岩, 俯冲早期地幔发生减压熔融形成弧前玄武岩, 其源区几乎没有俯冲板片物质和流体的参与, 之后被俯冲流体或熔体交代的亏损地幔发生部分熔融形成玻安岩, 二者可以作为板块起始俯冲的岩石学证据(Reagan等, 2010; Xia等, 2012; Li等, 2019). 除了较特殊的弧前位置外, 成熟俯冲带热结构主要与俯冲板片的年龄、俯冲速率、俯冲角度、俯冲带中的剪切加热速率以及地幔楔的性质有关(Syracuse等, 2010; Zheng, 2019). 在冷的俯冲带, 俯冲洋壳在弧前不会经历显著的脱水, 因此板片在弧下深度大量脱水交代上覆地幔楔, 然后受到加热发生熔融形成玄武岩(郑永飞等, 2016). 在热的俯冲带, 弧前已经脱水的洋壳在弧下深度不再大量脱水, 但俯冲板片的后撤可以诱发软流圈的侧向流动, 进而导致地幔楔底部和板片表面的解耦以及它们的温度升高(Kincaid和Griffiths, 2003), 这可以诱发弧后深度的板片熔融产生熔体交代地幔楔进而形成玄武岩(Zheng, 2019). 俯冲大洋板片回卷引起的地幔角流和弧下热的软流圈与冷的地幔楔之间的相互作用在弧岩浆的产生中发挥了至关重要的作用(例如, Hoernle等, 2008; Turner等, 2017; Zheng, 2019).

最新的全球后弧(rear-arc)火山岩的大数据分析发现, 俯冲组分交代之前的地幔楔的组成具有极度不均一性(Turner等, 2017); 在排除俯冲组分的影响之后, 作者认为其同位素变化可以用两个端元的混合来解释, 一个端元类似亏损的MORB地幔源区, 另一个富集端元则具有EMI的同位素特征, 并推断这个富集端元是软流圈低程度熔体交代的古老大陆岩石圈地幔, 而软流圈地幔楔角流将这种岩石圈地幔组分卷入到了弧下软流圈地幔中. 同样, 早期弧岩浆在岩石圈地幔中形成的辉石岩也可以与晚期软流圈来源的弧岩浆发生相互作用(Carlson等, 2018; Hickey-Vargas等, 2016). 事实上, 除了物质贡献之外, 弧下软流圈地幔角流带来的热在弧玄武质岩浆的产生中发挥了重要作用, 会导致地幔楔发生熔融产生玄武质岩浆(图7). 另外, 弧下复杂(垂直或平行海沟)的软流圈地幔楔角流会导致弧下地幔沿不同的方向发生物质流动, 改变弧下地幔的源区组成(例如, Hoernle等, 2008).

基于对世界上洋内弧和大陆弧玄武岩-安山岩样品的Fe同位素分析, Foden等(2018)揭示其Fe同位素组成与弧的热参数呈负相关. 热参数(即板片年龄与垂直俯冲速率的乘积, 用以表征俯冲板片温度与其几何形态参数的关系; Kirby等, 1996)高的弧下地幔经历了更强烈的角流和更大程度的熔体抽取, 因而亏损重Fe同位素. 扩散导致的动力学分馏对轻同位素的富集也有重要贡献. 这些岩石的Fe同位素变化主要与部分熔融和分离结晶有关, 其原始岩浆富集轻Fe同位素组成, 是源区亏损和俯冲交代的结果. 除了上述动力学机制, 板片的回卷、撕裂、断离或拆沉以及扩张洋脊俯冲、无震海岭或大洋高原俯冲、俯冲侵蚀等过程在弧岩浆岩的产生中也发挥了非常重要作用(王强等, 2020及其所引参考文献).

实验和数值模拟研究提出一种岛弧岩浆成因的底辟模式. 在板片俯冲过程中, 在板片与地幔楔的接触界面(即俯冲隧道)会发生蚀变洋壳、沉积物、蛇纹石化橄榄岩和地幔楔橄榄岩的机械混合, 从而形成混杂岩(Hall和Kincaid, 2001; Gerya和Yuen, 2003; Zhu等, 2009). 该混杂岩在浮力的作用下会底辟上升进入地幔楔热的核部, 发生部分熔融形成弧岩浆岩(Behn等, 2011; Marschall和Schumacher, 2012). 这种混杂岩部分熔融形成的熔体具有与实际观测的弧岩浆岩相似的地球化学特征(Castro等, 2010; Behn等, 2011; Marschall和Schumacher, 2012; Nielsen和Marschall, 2017; Codillo等, 2018; Cruz-Uribe等, 2018). 其中, 沉积物为主体的混杂岩部分熔融会形成钙碱性的玄武安山岩-安山岩序列(Cruz-Uribe等, 2018; Codillo等, 2018), 而蛇纹岩占主体的混杂岩部分熔融会产生岛弧拉斑玄武岩(Codillo等, 2018). 但是, 底辟的混杂岩如何进入相对较冷的地幔楔内部, 还是一个尚未解决的问题.

一些研究认为, 俯冲板片发生部分熔融形成熔体会交代地幔楔橄榄岩, 形成富斜方辉石辉石岩或二辉

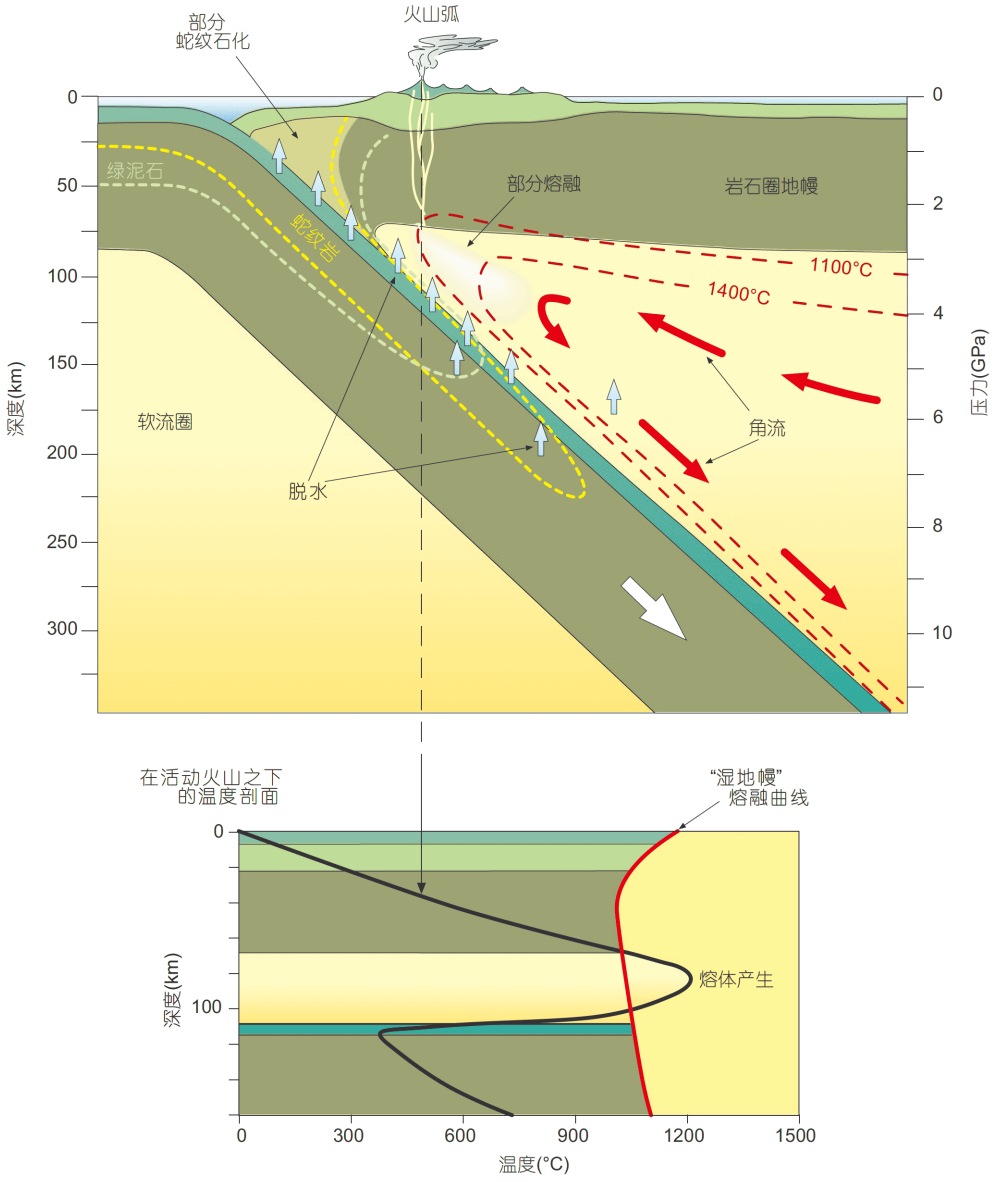


图 7　火山弧下的熔融过程

俯冲板片的脱水导致俯冲板片上盘蛇纹岩的形成和在更深度处热的软流圈地幔楔熔融形成弧岩浆岩. 据Stern(2000)和Frisch等(2011)

岩(Ertan和Leeman, 1996; Varfalvy等, 1996; Tamura和Arai, 2006), 这种辉石岩比橄榄岩更容易发生部分熔融. 因此, 在相同的温压条件下, 辉石岩的部分熔融会产生更多的熔体(Pertermann和Hirschmann, 2003; Hirschmann等, 2003; Lambart等, 2009), 并且辉石岩熔体与周围的地幔橄榄岩发生反应, 形成单斜辉石/角闪石脉体(Pilet等, 2008; Lambart等, 2012)或者Si不饱和的、高CaO/Al_2O_3(>1)的玄武质岩浆(Médard等, 2006; Sorbadere等, 2013a).

4.3　弧玄武质岩浆的演化与喷发

对弧玄武岩成因研究的一个重要起点是其原始成分的确定(Schmidt和Jagoutz, 2017; Zheng等, 2020). 原始岩浆成分与地幔橄榄岩(其中橄榄石的Fo(Mg/(Mg+Fe^{2+}))值=0.87~0.91, Ni含量=2000~4000ppm(Korenaga和Kelemen, 2000))平衡. 因此, 可以通过橄榄石-熔

体铁镁交换系数Kd(Fe/Mg)$^{ol/liq}$=0.30(Roeder和Emslie, 1970)来判别原始岩浆成分. $Mg^{\#}$=0.65~0.75和Ni=150~500ppm在岩石样品可视为原始岩浆, 一般原始岩浆岩在SiO_2=49wt%时, 其MgO≥9wt%. 与这些指标相比, 多数弧玄武质岩浆显然经历了结晶分异作用. 原始的弧玄武质岩浆具有很高的水含量(~4wt%)(Plank等, 2013)和低的黏度, 因而易于发生结晶分异作用, 仅仅很少的一部分能直接喷出地表, 这些特点使得自然界中的弧玄武岩并不具有类似于洋中脊、洋岛和大火成岩省玄武岩的规模(Rogers, 2015), 也决定了弧玄武质岩浆演化的诸多特殊性.

弧玄武岩浆的化学成分演化由矿物的结晶序列决定, 高的水含量能够有效降低斜长石的液相线, 延缓其首晶出现的时间(Sisson和Grove, 1993), 加之岩浆高的氧逸度能够促进铁钛氧化物的分异, 派生的熔体会向着FeO持续亏损的趋势演化, 即钙碱性分异趋势(Arculus, 2003; Zimmer等, 2010). Williams等(2018)研究发现, IBM洋内弧玄武岩-安山岩的Fe同位素分馏受控于多阶段的岩浆分异, 从第一阶段的橄榄石和辉石的结晶, 到第二阶段的磁铁矿结晶再到最后硫化物结晶, Fe同位素分馏各不相同. 不同于贫水的洋岛拉斑质玄武岩, 弧玄武岩的演化对压力十分敏感(Cashman和Edmonds, 2019). 例如, 在恒压降温过程中, 高压条件下, 熔体成分演化受镁铁质矿物相的结晶控制, 并伴随MgO的急剧降低和Al_2O_3的增加, 但K_2O的升高幅度却非常有限(图8a和8b). 斜长石饱和时熔体的MgO含量与压力呈线性关系, 并被熔体演化过程中最大的Al_2O_3含量这一指标所记录(图8b); MgO-K_2O演化曲线斜率的突然增大则表明了岩浆结晶度的增加. 恒温降压过程中熔体演化的趋势则不同, 从降压导致的辉石溶解开始, 熔体的MgO反而会增加, 随后则是Al_2O_3的急剧降低和K_2O的快速升高, 这些指标记录了广泛的降压驱动的斜长石结晶(图8c和8d). 另外, 岩浆上升过程中也会因为去气作用改变熔体的演化趋势(Blundy等, 2006).

相比于高黏度硅质岩浆的灾害性喷发, 弧玄武质岩浆更多的以小规模溢流式喷发为主, 尤其是在静水压力较大的海底环境(Branney和Acocella, 2015). 然而,

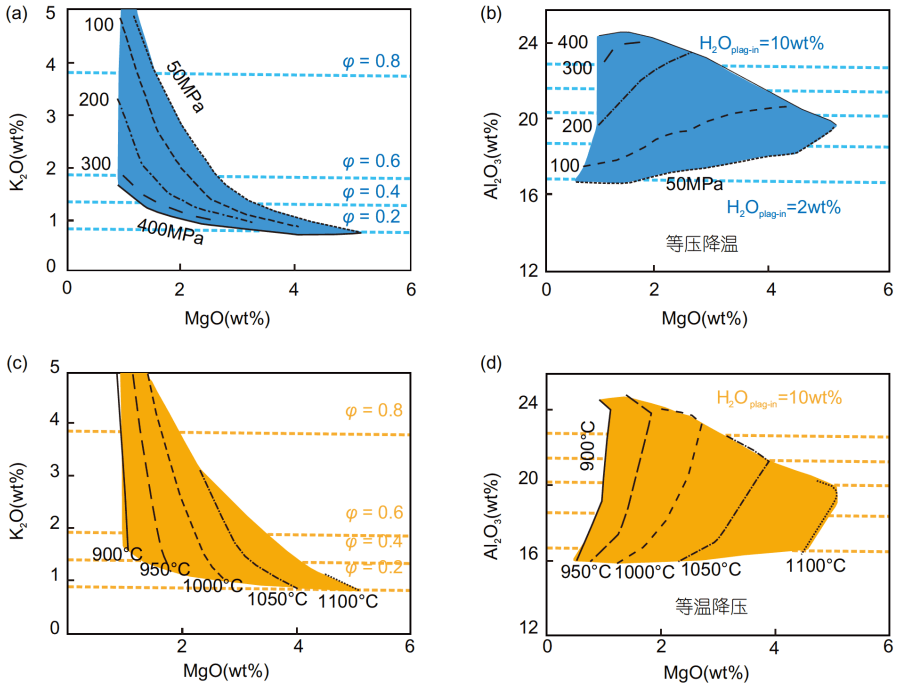


图 8　富水弧玄武岩在恒压降温过程(a和b)和恒温降压(c和d)过程中熔体成分的演化趋势

(a)和(c)K_2O/MgO, 并标注了结晶度(φ)和压力. (b)和(d)MgO/Al_2O_3, 并标注了压力. 初始岩浆成分为1974年富埃戈(Fuego)喷发的火山岩的全岩成分, 含4.5wt% H_2O, 氧逸度为NNO缓冲体系. 用"rhyolite-MELTS"模拟了熔体成分的演化过程, 压力从400MPa下降至50MPa, 温度从1100℃降低至900℃. 成分区间覆盖了富埃戈火山绝大部分观察到的熔体成分, 并且在一个复杂的岩浆系统内, 单次喷发记录的岩浆成分区间在不同的压力-温度条件下会增大. 据Cashman和Edmonds(2019)

在马里亚纳弧Rota-1火山则首次观察到了海底玄武质火山的爆炸式喷发(Chadwick等, 2008). H_2O对弧玄武质岩浆喷发的控制作用一直备受关注, 但越来越多的研究则强调CO_2对岩浆动力学过程的影响(Collins等, 2009; Blundy等, 2010; Caricchi等, 2018). 由于岩浆动能的约束, 大部分的玄武质岩浆都经历了中上地壳的储存, 然后才能喷发出地表(Cashman和Edmonds, 2019), 但也存在直接从地幔起源快速上升喷发的实例(Ruprecht和Plank, 2013). 近年来微束分析技术的发展, 使得定量刻画弧玄武质岩浆动力学过程的时间尺度成为现今研究的热点之一(例如, Lynn等, 2018; Ruth等, 2018).

5　存在问题与研究展望

尽管弧玄武岩的研究取得了许多重要进展, 但仍有许多科学问题亟待解决. 建议在未来研究中重点关注以下四个方向.

5.1　弧下地幔交代作用与弧岩浆源区的形成

前面提到, 俯冲板片释放流体或熔融产生的熔体交代弧下地幔楔, 形成弧玄武岩的地幔源区. 实际上, 俯冲板片的成分非常复杂, 除了玄武质洋壳外, 还包括其上覆的海底沉积物(含碳酸岩和陆源沉积物)和下覆大洋岩石圈地幔. 此外, 增生楔沉积物或俯冲带上盘的物质也可能通过俯冲、拖曳或俯冲底侵、俯冲侵蚀等过程进入地幔楔底部. 上述物质本身可能含水(如沉积物), 或经过绿泥石化、蛇纹石化或角闪石化, 这些富水岩石在俯冲过程中可携带大量的水进入到地幔. 因此, 由于流体或熔体来源和成分的复杂性, 其对弧下地幔的交代作用比原来想象的要复杂得多. 以弧环境中出现橄榄玄粗质岩石或硅不饱和的富钾岩石(富钾镁铁质岩)为例, 其富集幔源区的形成过程一直存在激烈的争议: 有些学者认为, 俯冲的含沉积物大洋板片进变质到榴辉岩相时将K保存在多硅白云母中, 只有在多硅白云母分解或者参与部分熔融之后, 大量的K才会被释放进入到地幔楔中并交代地幔, 形成富K的地幔源区, 富K地幔熔融最终形成富钾火山岩(Schmidt, 1996, 2015; Conticelli等, 2009; Spandler和Pirard, 2013). 而另一些学者基于橄榄岩和含水沉积物熔体的混合物的熔融实验, 提出沉积物部分熔融形成的富硅熔体与地幔橄榄岩发生反应后, 也可以逐渐演化为类似俯冲带的富钾玄武质熔体(Mallik等, 2015, 2016). 两种观点都强调了俯冲沉积物组分是K的主要来源, 但是参与弧岩浆演化的方式存在区别.

不同性质熔体与地幔橄榄岩反应的产物受熔体成分、熔体与地幔橄榄岩比例、反应的温压条件等多种因素控制. Si饱和的岩浆或者高Si活度系数(αSiO_2)的岩浆与橄榄岩反应时, 熔体与橄榄岩反应式可总结为(Johnston和Wyllie, 1989; Rapp等, 1999; Lambart等, 2012; Mallik和Dasgupta, 2012; Wang等, 2016; Wang等, 2019):

熔体1+橄榄石=斜方辉石+富Al相±熔体2;

低Si活度系数(αSiO_2)的岩浆与橄榄岩反应时反应式可总结为(Morgan和Liang, 2003; Beck等, 2006; Tursack和Liang, 2012; Lambart等, 2012; Saper和Liang, 2014):

熔体1+斜方辉石=橄榄石+富Al相+单斜辉石+熔体2;

斜方辉石耗尽后反应变为:

熔体1+橄榄石=单斜辉石+富Al相±熔体2;

其中, 反应进行的程度取决于熔体-橄榄岩比例(例如, Rapp等, 1999), 如果熔/岩比例小, 只会交代少量橄榄岩; 如果熔/岩比例大, 除了发生地幔交代作用, 反应后的残余熔体喷出地表而形成岛弧岩石. 根据初始反应熔体的差异, 反应后的熔体成分包括高$Mg^{\#}$安山岩-英安岩、玻安岩、碱性玄武岩、拉斑玄武岩和超钾质岩等多种岩石类型(Carroll和Wyllie, 1989; Lambart等, 2012; Mallik和Dasgupta, 2012; Mallik等, 2015, 2016). 富Al相矿物主要为石榴子石、尖晶石和斜长石, 受控于反应压力, 高压时为石榴子石, 低压条件下为尖晶石甚至斜长石(Lambart等, 2012; Saper和Liang, 2014). 如果熔体富K, 反应产物中可产生少量的金云母(Woodland等, 2018). 当熔体含水量高时会交代地幔岩石形成角闪石(Gervasoni等, 2017; Corgne等, 2018). 研究揭示, 熔体/地幔岩石比例在俯冲带壳幔相互作用过程中发挥了关键作用: 一方面有效地控制交代反应的岩石学过程, 形成不同类型的地幔交代岩, 其易熔特征可促进地幔部分熔融, 成为俯冲带岩浆的重要源区; 另一方面显著影响岛弧岩浆的成分特征, 促进弧岩浆的演化和大陆地壳的生长(Su等, 2019; Zheng等, 2020).

另外, 在火山弧之下的板片深度, 板片来源的俯冲

组分可以是超临界流体(Kessel等, 2005; Mibe等, 2011; Kawamoto等, 2012). 这是因为随着温压增加(第二临界端点之上), 富水流体和含水硅酸盐熔体变得完全混溶成为一相存在, 因而具有类似熔体的元素迁移能力(Kessel等, 2005). 虽然在该相中水和硅酸盐的含量大都介于30~70wt%(Ni等, 2017), 但是只有当富水流体与含水熔体之间达到完全混溶后才会具有强大的溶解元素能力(Zheng, 2019). 即使超临界流体可以, 但是它在地幔深度不易保存, 在弧下地幔上升的过程中, 降压会导致其再次分解成富水流体和含水硅酸盐熔体(Kawamoto等, 2012), 这可能是现今观察到的弧玄武岩地幔源区含有多种俯冲组分的原因.

除了上述富水流体或含水熔体地幔交代作用外, 俯冲带含CO_2流体或碳酸岩熔体对地幔也有交代作用, 但是俯冲板片的脱碳机制以及对弧玄武岩的贡献目前还存在较大争议. 岛弧玄武岩中熔体包裹体和火山气体的研究表明, 原始的岛弧玄武岩至少含有>3000ppm的CO_2(Wallace, 2005; Blundy等, 2010). 对弧下地幔捕虏体(如勘察加半岛弧, Kepezhinskas和Defant, 1996)的研究也表明, 俯冲的碳酸岩会与地幔楔橄榄岩发生反应形成富集磷灰石、角闪石和金云母等交代矿物的二辉橄榄岩或交代脉体. 这些岩石学证据表明, 板片俯冲伴随着明显的脱碳过程(Sano和Williams, 1996). 然而, 相平衡模拟实验和热力学模型预测, 由于俯冲板片太冷, 在俯冲过程中并不能发生明显的碳酸岩分解、变质脱碳及沉积物/洋壳部分熔融等脱碳过程(Dasgupta等, 2004, 2005; Thomsen和Schmidt, 2008; Tsuno和Dasgupta, 2011, 2012; Thomson等, 2016), 大量的俯冲碳酸岩会俯冲进入深部地幔. 这与岛弧玄武岩高CO_2含量及弧下地幔碳酸岩交代的岩石学证据不相符. 事实上, 镁铁碳酸盐矿物在弧玄武质岩浆源区80~160km深度仍稳定存在, 直至地幔过渡带才发生明显的脱碳(Dasgupta, 2013; Thomson等, 2016). Dasgupta(2013)提出了混杂岩底辟、富H_2O+CO_2沉积物分解/熔融和热俯冲三种可能的机制来解释这种差异. 新的实验岩石学和野外观察支持富水沉积物在脱流体过程中会促进碳酸岩的分解, 使得俯冲板片在较浅的深度就可以发生明显的脱碳作用(Gorman等, 2006; Frezzotti等, 2011; Ague和Nicolescu, 2014; Duncan和Dasgupta, 2014), 这种潜在的机制可能是岛弧玄武岩具高CO_2含量的原因之一.

5.2 弧玄武岩的产生与岩浆储库演化

一般认为, 俯冲带地幔楔橄榄岩的熔融与俯冲大洋板片析出的挥发分组分的加入有关(Tatsumi等, 1986; Tatsumi, 2005). 在洋中脊, 软流圈地幔上涌并伴随压力降低, 地幔岩石穿过其固相线, 发生部分熔融(Klein和Langmuir, 1987). 这种减压熔融模式也可用来解释俯冲带弧下地幔的熔融(Tatsumi等, 1983, Plank和Langmuir, 1988). 某些岛弧玄武岩岩浆具有非常低的水含量, 与缺水条件下地幔橄榄岩减压熔融模式相吻合(Elkins-Tanton等, 2001). 但是, 相对固态的地幔楔如何发生减压作用, 则是个尚未解决的问题. 只有部分岛弧环境下软流圈地幔上涌进入减薄的地幔楔, 在高温缺水的条件下发生降压熔融. 例如在日本岛弧, 快速的高角度大洋俯冲和日本海弧后盆地的打开导致软流圈地幔上涌, 从而发生弧后地幔减压熔融(Tatsumi等, 1983). 除减压熔融以外, 需要其他熔融模式来解释俯冲带的富水岩浆, 包括水致熔融和含水等温降压熔融(图9). 无论哪种过程, 地幔橄榄岩精确的湿固相线温度的确立对揭示弧玄武质岩浆的产生机制非常关键. 但目前为止, 不同实验得到的橄榄岩湿固相线温度差别很大. 因此, 不同温压下地幔橄榄岩湿固相线温度的精确确定是一个亟待解决的重要科学问题.

特殊的岛弧玄武岩的形成往往需要特殊的地幔交代过程或动力学机制. 如前面提到的在岛弧中出现的

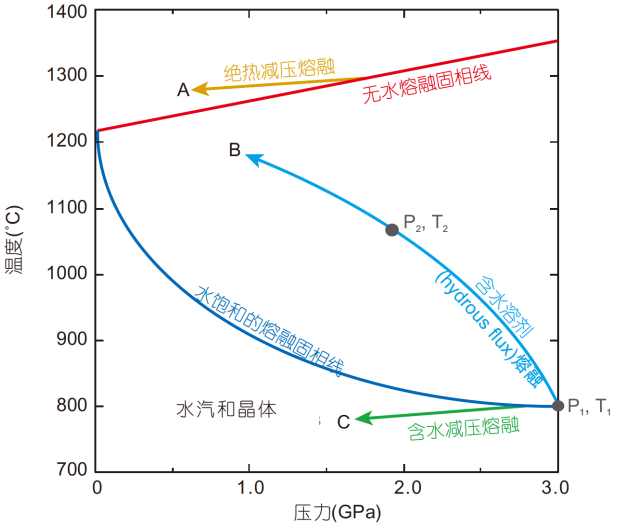


图 9　三种地幔熔融过程的温度-压力图

A, 减压熔融; B, 含水溶剂熔融; C, 含水等温降压熔融. 修改自Gaetani和Grove(2003)

洋岛型玄武岩，其可能来自俯冲板片熔体交代地慢楔、地幔楔中富集组分的熔融、深部上涌地幔等源区，但其形成的动力学机制可能包括洋脊俯冲或者板片撕裂形成的板片窗环境(Mullen和Weis, 2013; Thorkelson等, 2011)，或者深部地幔上涌，类似地幔柱等(Nakajima和Hasegawa, 2007)，或者弧后深度地幔交代岩的部分熔融. 具MORB型特征的弧玄武岩的形成也常与洋脊俯冲形成的板片窗环境有关(Cole和Stewart, 2009).

玄武质岩浆产生后，其在上升穿过地幔、进入地壳并在最终喷出地表的过程中，要经历一系列的演化过程. 传统的观点认为，弧玄武岩-安山岩-英安岩-流纹岩的组合主要由俯冲含水流体触发的幔源玄武质岩浆作用在岩浆房或上升途中发生分离结晶、地壳混染与分离结晶(AFC)或熔融-同化-存储-均一(MASH)过程所控制. 但是，近年来大量的研究显示，地壳内的岩浆储库大部分时间以晶粥体形式存在，而非传统认为的富熔体相岩浆房(例如，Cooper和Kent, 2014; Cashman等, 2017). 由于岩浆在冷的浅部地壳中易于发生热丢失，以及降压结晶导致的黏度障碍(Annen等, 2006)，单批次垂向的岩浆脉冲并不具有喷发能力，因而供给大型火山喷发，尤其是超级火山，需要在中上地壳形成一定规模的岩浆储库(Bachmann和Bergantz, 2008). 因此，对于喷出到地表的玄武岩，其成分的演化不仅需要研究其地幔源区，也需要深入探究其喷发前岩浆的演化过程. 以弧高铝玄武岩为例，主流的观点认为该类岩石来自富水玄武岩的分离结晶，但是一些实验研究表明，在高压(0.7~1.2GPa)条件下，无水玄武质岩浆的长石结晶也会受到抑制(Gust和Perfit, 1987; Draper和Johnston, 1992; Husen等, 2016; Villiger等, 2004)，即辉石优于长石先结晶，所以一些无水的岩浆也有可能分异形成Al_2O_3含量较高的玄武岩(Gust和Perfit, 1987; Draper和Johnston, 1992; Villiger等, 2004). 有研究在洋中脊地区发现了由辉石高压分离结晶形成的无水拉斑质高铝玄武岩(Eason和Sinton, 2006).

5.3　弧玄武质岩浆作用与物质循环

俯冲带是地球物质循环的重要场所，被称为“俯冲工厂”(Tatsumi, 2005). 在俯冲过程中，大洋板片的沉积物、洋壳以及地幔岩石圈通过俯冲作用和俯冲上盘一些物质通过拖曳、俯冲侵蚀等过程进入到地幔中，这些物质释放的流体或熔融产生的熔体交代地幔楔橄榄岩或其本身同地幔混合形成弧岩浆岩的源区，然后弧岩浆作用再将进入到弧下地幔的组分带回到地表(图10). 正常的弧玄武岩一般具有富集LILE和LREE, 亏损HFSE和HREE的特点(图3)，主要与俯冲流体对地幔楔橄榄岩的交代有关(例如, Tatsumi, 2005; Zheng, 2019). 根据实验岩石学数据和水含量的估计, Tatsumi和Kogiso(2003)提出岛弧玄武岩的“弧特征”可以通过俯冲板片和沉积物通过脱水作用的流体加入地幔楔来解释. 另外, 大量的资料显示, 俯冲沉积物、玄武质洋壳甚至俯冲上盘物质的熔体组分都可能通过弧岩浆作用而循环回到地壳中(Peacock等, 1994; Elliott等, 1997; Kay等, 2005; 王强等, 2020; Zheng等, 2020), 甚至许多岛弧玄武岩中含有大量上覆岛弧地壳物质组分. 比如 Nd-Hf同位素研究认为，中墨西哥岛弧玄武岩的地幔源区不是俯冲海沟沉积物，而是循环的弧前俯冲侵蚀的花岗闪长岩(Straub等, 2015). 因此, 如何有效识别弧玄武岩中不同循环组分的信息，特别是估算俯冲带物质(如碳、地壳)通量(图10)，仍然是当前国际地质的一个研究难点.

5.4　弧玄武岩产生的动力学机制与板块构造的启动

“将今论古”是地质学研究最基本原理之一. 大量的研究将太古代的岩浆岩同现代弧岩浆岩进行对比，提出板块构造活动(即洋壳俯冲)在太古代已经出现，其启动时间包括3.0~2.5、3.5~2.5和>3.5Ga等(Shir-

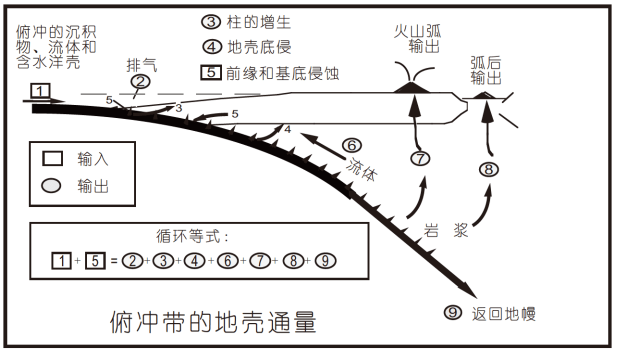


图 10　俯冲带物质循环示意图

1, 输入的沉积物、流体和含水洋壳; 2, 排气; 3, 柱的增生; 4, 地壳底侵; 5, 前缘和基底侵蚀; 6, 俯冲板片释放流体; 7, 火山弧输出; 8, 弧后岩浆输出; 9, 返回地幔. 修改自Scholl等(1994)

ey和Hanson, 1984; Smithies等, 2003, 2004; Martin等, 2005, 2014; Hastie等, 2015). 板块构造启动时间争论的一个核心问题是, 具有类似现代俯冲机制(即具有地幔楔的俯冲带)的板块构造体制是何时出现的?

在新生代俯冲带, 大洋板片的俯冲不仅形成了地幔楔结构, 还产生了起源于地幔楔的弧玄武岩(图3), 或板片熔体与地幔楔相互作用后形成的高Nb或富Nb玄武岩、高镁安山岩(赞岐岩)、埃达克岩等(王强等, 2020及其所引参考文献). 有研究发现, 一些形成于3.0 Ga左右的玄武岩或玄武质岩石富集LILE、亏损HFSE, 提出类似现代俯冲机制(含地幔楔)的板块构造过程在3.0Ga已经启动(Smithies等, 2003, 2004). 与此类似, 部分研究者根据晚太古代(3.0~2.5Ga)出现了类似现代弧环境的玻安岩-高镁安山岩(赞岐岩)-富Nb玄武岩-埃达克岩等组合, 认为俯冲大洋板片熔融产生的熔体与地幔楔橄榄岩发生了强烈相互作用, 提出类似现代俯冲机制的板块构造过程至少在晚太古代已经启动(例如, Polat和Kerrich, 2002; Smithies等, 2004; Martin等, 2005, 2014).

Turner等(2014)发现, 加拿大魁北克的努夫亚吉图克(Nuvvuagittuq)4.4或3.8Ga绿岩带的火山地层序列和地球化学特征完全可以与象征现代俯冲机制的IBM弧的火山地层序列对比, 这套地层中的玄武岩具有类似于弧前玄武岩的平坦稀土和HFSE分布型式, 其形成与岩石圈初始破裂、软流圈减压熔融相关, 而努夫亚吉图克绿岩带高钛玄武岩与IBM的前弧玄武岩具有相似的地球化学特征, 其来源于由于俯冲洋壳断裂导致的软流圈地幔减压熔融, 从而提出板块构造可能始于4.4或3.8Ga. Furnes等(2013)根据南非古太古代(3.5~3.3Ga)的Onverwacht绿岩带中大量的玄武岩有明显的负Nb和Ta异常和富集LILE的特点, 指出其起源于弧下交代地幔橄榄岩的部分熔融. 因此, 在太古宙早期似乎就已经存在了类似现代俯冲机制的板块构造体制. 但是, 上述研究推论还需要构造、沉积和高压-超高压变质等其他证据的支持. 因此, 弧玄武岩产生的动力学机制与板块构造的启动仍旧是当前国际地质的尚未解决的一个热点问题.

致谢 感谢郑永飞院士邀请撰写本文. 郑永飞院士、宋述光教授和三位匿名审稿人提供了建设性修改建议.

参考文献

王强, 唐功建, 郝露露, Wyman D, 马林, 但卫, 张修政, 刘金恒, 黄彤宇, 许传兵. 2020. 洋中脊或海岭俯冲与岩浆作用及金属成矿. 中国科学: 地球科学, 50: 1401–1423

吴福元, 王建刚, 刘传周, 刘通, 张畅, 纪伟强. 2019. 大洋岛弧的前世今生. 岩石学报, 35: 1–15

徐义刚. 1999. 拉张环境中的大陆玄武岩浆作用: 性质及动力学过程. 见: 郑永飞, 等, 主编. 化学地球动力学进展. 北京: 科学出版社. 119–167

郑永飞, 陈仁旭, 徐峥, 张少兵. 2016. 俯冲带中的水迁移. 中国科学: 地球科学, 46: 253–286

郑永飞, 陈伊翔, 戴立群, 赵子福. 2015. 发展板块构造理论: 从洋壳俯冲带到碰撞造山带. 中国科学: 地球科学, 45: 711–735

Agostini S, Ryan J G, Tonarini S, Innocenti F. 2008. Drying and dying of a subducted slab: Coupled Li and B isotope variations in Western Anatolia Cenozoic volcanism. Earth Planet Sci Lett, 272: 139–147

Ague J J, Nicolescu S. 2014. Carbon dioxide released from subduction zones by fluid-mediated reactions. Nat Geosci, 7: 355–360

Aguillón-Robles A, Calmus T, Benoit M, Bellon H, Maury R C, Cotten J, Bourgois J, Michaud F. 2001. Late Miocene adakites and Nb-enriched basalts from Vizcaino Peninsula, Mexico: Indicators of East Pacific Rise subduction below Southern Baja California? Geology, 29: 531–534

Annen C, Blundy J D, Sparks R S J. 2006. The genesis of intermediate and silicic magmas in deep crustal hot zones. J Petrol, 47: 505–539

Arculus R J. 2003. Use and abuse of the terms calcalkaline and calcalkalic. J Petrol, 44: 929–935

Bachmann O, Bergantz G. 2008. The magma reservoirs that feed supereruptions. Elements, 4: 17–21

Bacon C R, Bruggman P E, Christiansen R L, Clynne M A, Donnelly-Nolan J M, Hildreth W. 1997. Primitive magmas at five cascade volcanic fields: Melts from hot, heterogeneous sub-arc mantle. Can Mineral, 35: 397–423

Baker M B, Grove T L, Price R. 1994. Primitive basalts and andesites from the Mt. Shasta region, N. California: Products of varying melt fraction and water content. Contrib Mineral Petrol, 118: 111–129

Beard J S, Lofgren G E. 1992. An experiment-based model for the petrogenesis of high-alumina basalts. Science, 258: 112–115

Beate B, Monzier M, Spikings R, Cotten J, Silva J, Bourdon E, Eissen J P. 2001. Mio-Pliocene adakite generation related to flat subduction in southern Ecuador: The Quimsacocha volcanic center. Earth Planet Sci Lett, 192: 561–570

Beaumais A, Bertrand H, Chazot G, Dosso L, Robin C. 2016. Temporal magma source changes at gaua volcano, vanuatu island arc. J Volcanol Geotherm Res, 322: 30–47

Beccaluva L, Bianchini G, Mameli P, Natali C. 2013. Miocene shoshonite volcanism in Sardinia: Implications for magma sources and geodynamic evolution of the central-western Mediterranean. Lithos, 180-181: 128–137

Beck A R, Morgan Z T, Liang Y, Hess P C. 2006. Dunite channels as viable pathways for mare basalt transport in the deep lunar mantle. Geophys Res Lett, 33: L01202

Behn M D, Kelemen P B, Hirth G, Hacker B R, Massonne H J. 2011. Diapirs as the source of the sediment signature in arc lavas. Nat Geosci, 4: 641–646

Bénard A, Ionov D A. 2013. Melt- and fluid-rock interaction in supra-subduction lithospheric mantle: Evidence from Andesite-hosted veined peridotite xenoliths. J Petrol, 54: 2339–2378

Benton L D, Ryan J G, Savov I P. 2004. Lithium abundance and isotope systematics of forearc serpentinites, Conical Seamount, Mariana forearc: Insights into the mechanics of slab-mantle exchange during subduction. Geochem Geophys Geosyst, 5: Q08J12

Blatter D L, Sisson T W, Hankins W B. 2013. Crystallization of oxidized, moderately hydrous arc basalt at mid- to lower-crustal pressures: Implications for andesite genesis. Contrib Mineral Petrol, 166: 861–886

Bloomer S H, Stern R J, Fisk E, Geschwind C H. 1989. Shoshonitic volcanism in the northern Mariana arc: 1. Mineralogic and major and trace element characteristics. J Geophys Res, 94: 4469–4496

Blundy J, Cashman K V, Rust A, Witham F. 2010. A case for CO_2-rich arc magmas. Earth Planet Sci Lett, 290: 289–301

Blundy J, Cashman K, Humphreys M. 2006. Magma heating by decompression-driven crystallization beneath andesite volcanoes. Nature, 443: 76–80

Bourdon E, Eissen J P, Gutscher M A, Monzier M, Hall M L, Cotten J. 2003. Magmatic response to early aseismic ridge subduction: The Ecuadorian margin case (South America). Earth Planet Sci Lett, 205: 123–138

Bouvier A S, Métrich N, Deloule E. 2008. Slab-derived fluids in magma sources of St. Vincent (Lesser Antilles Arc): Volatile and light element imprints. J Petrol, 49: 1427–1448

Bouvier A S, Métrich N, Deloule E. 2010. Light elements, volatiles, and stable isotopes in basaltic melt inclusions from Grenada, Lesser Antilles: Inferences for magma genesis. Geochem Geophys Geosyst, 11: Q09004

Branney M, Acocella V. 2015. Calderas. In: Sigurdsson H, Houghton B F, Mcnutt S R, Rymer H, Stix J, Mcbirney A R, eds. The Encyclopedia of Volcanoes. London: Academic Press. 299–315

Brenan J M, Shaw H F, Ryerson F J, Phinney D L. 1995. Mineral-aqueous fluid partitioning of trace elements at 900°C and 2.0 GPa: Constraints on the trace element chemistry of mantle and deep crustal fluids. Geochim Cosmochim Acta, 59: 3331–3350

Brophy J G. 1989. Can high-alumina arc basalt be derived from low-alumina arc basalt? Evidence from Kanaga Island, Aleutian Arc, Alaska. Geology, 17: 333–336

Brophy J G, Marsh B D. 1986. On the origin of high-alumina arc basalt and the mechanics of melt extraction. J Petrol, 27: 763–789

Caricchi L, Sheldrake T E, Blundy J. 2018. Modulation of magmatic processes by CO_2 flushing. Earth Planet Sci Lett, 491: 160–171

Carlier G, Lorand J P, Liégeois J P, Fornari M, Soler P, Carlotto V, Cárdenas J. 2005. Potassic-ultrapotassic mafic rocks delineate two lithospheric mantle blocks beneath the southern Peruvian Altiplano. Geology, 33: 601–604

Carlson R W, Grove T L, Donnelly-Nolan J M. 2018. Origin of primitive tholeiitic and calc-alkaline basalts at Newberry Volcano, Oregon. Geochem Geophys Geosyst, 19: 1360–1377

Carroll M R, Wyllie P J. 1989. Experimental phase relations in the system tonalite-peridotite-H_2O at 15 kb: Implications for assimilation and differentiation processes near the crust-mantle boundary. J Petrol, 30: 1351–1382

Cashman K V, Edmonds M. 2019. Mafic glass compositions: A record of magma storage conditions, mixing and ascent. Philos Trans R Soc A-Math Phys Eng Sci, 377: 20180004

Cashman K V, Sparks R S J, Blundy J D. 2017. Vertically extensive and unstable magmatic systems: A unified view of igneous processes. Science, 355: eaag3055

Castillo P R, Rigby S J, Solidum R U. 2007. Origin of high field strength element enrichment in volcanic arcs: Geochemical evidence from the Sulu Arc, southern Philippines. Lithos, 97: 271–288

Castillo P R, Solidum R U, Punongbayan R S. 2002. Origin of high field strength element enrichment in the Sulu Arc, southern Philippines, revisited. Geology, 30: 707–710

Castro A, Gerya T, Garcia-Casco A, Fernandez C, Diaz-Alvarado J, Moreno-Ventas I, Low I. 2010. Melting Relations of MORB-Sediment Melanges in Underplated Mantle Wedge Plumes; Implications for the Origin of Cordilleran-type Batholiths. J Petrol, 51: 1267–1295

Chadwick Jr W W, Cashman K V, Embley R W, Matsumoto H, Dziak R P, de Ronde C E J, Lau T K, Deardorff N D, Merle S G. 2008. Direct video and hydrophone observations of submarine explosive eruptions at NW Rota-1 volcano, Mariana arc. J Geophys Res, 113: B08S10

Chan L H, Leeman W P, You C F. 2002. Lithium isotopic composition of Central American Volcanic Arc lavas: Implications for modification of subarc mantle by slab-derived fluids: Correction. Chem Geol, 182: 293–300

Codillo E A, Le Roux V, Marschall H R. 2018. Arc-like magmas generated by mélange-peridotite interaction in the mantle wedge. Nat Commun, 9: 2864

Cole R B, Stewart B W. 2009. Continental margin volcanism at sites of spreading ridge subduction: Examples from southern Alaska and western California. Tectonophysics, 464: 118–136

Collins S J, Pyle D M, Maclennan J. 2009. Melt inclusions track pre-eruption storage and dehydration of magmas at Etna. Geology, 37: 571–574

Conticelli S, Marchionni S, Rosa D, Giordano G, Boari E, Avanzinelli R. 2009. Shoshonite and sub-alkaline magmas from an ultrapotassic volcano: Sr-Nd-Pb isotope data on the Roccamonfina volcanic rocks, Roman Magmatic Province, Southern Italy. Contrib Mineral Petrol, 157: 41–63

Cooper K M, Kent A J R. 2014. Rapid remobilization of magmatic crystals kept in cold storage. Nature, 506: 480–483

Corgne A, Schilling M E, Grégoire M, Langlade J. 2018. Experimental constraints on metasomatism of mantle wedge peridotites by hybridized adakitic melts. Lithos, 308-309: 213–226

Crawford A J, Falloon T J, Eggins S. 1987. The origin of island arc high-alumina basalts. Contrib Mineral Petrol, 97: 417–430

Cruz-Uribe A M, Marschall H R, Gaetani G A, Le Roux V. 2018. Generation of alkaline magmas in subduction zones by partial melting of mélange diapirs—An experimental study. Geology, 46: 343–346

Dasgupta R, Hirschmann M M, Dellas N. 2005. The effect of bulk composition on the solidus of carbonated eclogite from partial melting experiments at 3 GPa. Contrib Mineral Petrol, 149: 288–305

Dasgupta R, Hirschmann M M, Withers A C. 2004. Deep global cycling of carbon constrained by the solidus of anhydrous, carbonated eclogite under upper mantle conditions. Earth Planet Sci Lett, 227: 73–85

Dasgupta R. 2013. Ingassing, storage, and outgassing of terrestrial carbon through geologic time. Rev Mineral Geochem, 75: 183–229

De Hoog J C, Savov I P. 2017. Boron isotopes as a tracer of subduction zone processes. In: Boron Isotopes. Berlin Heidelberg: Springer. 217–247

DeBari S M, Taylor B, Spencer K, Fujioka K. 1999. A trapped Philippine Sea plate origin for MORB from the inner slope of the Izu-Bonin trench. Earth Planet Sci Lett, 174: 183–197

Defant M J, Kepezhinskas P. 2001. Evidence suggests slab melting in arc magmas. Eos Trans AGU, 82: 65–80

Defant M J, Drummond M S. 1990. Derivation of some modern arc magmas by melting of young subducted lithosphere. Nature, 347: 662–665

Defant M J, Jackson T E, Drummond M S, de Boer J Z, Bellon H, Feigenson M D, Maury R C, Stewart R H. 1992. The geochemistry of young volcanism throughout western Panama and southeastern Costa Rica: An overview. J Geol Soc, 149: 569–579

Defant M J, Kepezhinskas P, Defant M J, Xu J F, Kepezhinskas P, Wang Q, Zhang Q, Xiao L. 2002. Adakites: Some variations on a theme. Acta Petrol Sin, 18: 129–142

Defant M J, Richerson P M, de Boer J Z, Stewart R H, Maury R C, Bellon H, Drummond M S, Feigenson M D, Jackson T E. 1991. Dacite genesis via both slab melting and differentiation: Petrogenesis of La Yeguada Volcanic Complex, Panama. J Petrol, 32: 1101–1142

Draper D S, Johnston A D. 1992. Anhydrous pt phase relations of an aleutian high-mgo basalt: An investigation of the role of olivine-liquid reaction in the generation of arc high-alumina basalts. Contrib Mineral Petrol, 112: 501–519

Duncan M S, Dasgupta R. 2014. CO_2 solubility and speciation in rhyolitic sediment partial melts at 1.5–3.0 GPa—Implications for carbon flux in subduction zones. Geochim Cosmochim Acta, 124: 328–347

Eason D, Sinton J. 2006. Origin of high-Al N-MORB by fractional crystallization in the upper mantle beneath the Galápagos Spreading Center. Earth Planet Sci Lett, 252: 423–436

Elburg M, Foden J. 1999. Sources for magmatism in central sulawesi: Geochemical and Sr-Nd-Pb isotopic constraints. Chem Geol, 156: 67–93

Elkins-Tanton L T, Grove T L, Donnelly-Nolan J. 2001. Hot, shallow mantle melting under the cascades volcanic arc. Geology, 29: 631–634

Elliott T, Plank T, Zindler A, White W, Bourdon B. 1997. Element transport from slab to volcanic front at the mariana arc. J Geophys Res, 102: 14991–15019

Ertan I E, Leeman W P. 1996. Metasomatism of Cascades subarc mantle: Evidence from a rare phlogopite orthopyroxenite xenolith. Geology, 24: 451–454

Falloon T J, Danyushevsky L V, Crawford T J, Maas R, Woodhead J D, Eggins S M, Bloomer S H, Wright D J, Zlobin S K, Stacey A R. 2007. Multiple mantle plume components involved in the petrogenesis of subduction-related lavas from the northern termination of the Tonga Arc and northern Lau Basin: Evidence from the geochemistry of arc and backarc submarine volcanics. Geochem Geophys Geosyst, 8: Q09003

Foden J, Sossi P A, Nebel O. 2018. Controls on the iron isotopic composition of global arc magmas. Earth Planet Sci Lett, 494: 190–201

Foley S F, Barth M G, Jenner G A. 2000. Rutile/melt partition coefficients for trace elements and an assessment of the influence of

rutile on the trace element characteristics of subduction zone magmas. Geochim Cosmochim Acta, 64: 933–938

Freymuth H, Elliott T, van Soest M, Skora S. 2016. Tracing subducted black shales in the Lesser Antilles arc using molybdenum isotope ratios. Geology, 44: 987–990

Freymuth H, Vils F, Willbold M, Taylor R N, Elliott T. 2015. Molybdenum mobility and isotopic fractionation during subduction at the Mariana arc. Earth Planet Sci Lett, 432: 176–186

Frezzotti M L, Selverstone J, Sharp Z D, Compagnoni R. 2011. Carbonate dissolution during subduction revealed by diamond-bearing rocks from the Alps. Nat Geosci, 4: 703–706

Frisch W, Meschede M, Blakey R. 2011. Plate Tectonics: Continental Drift and Mountain Building. Berlin Heidelberg: Springer. 212

Furnes H, de Wit M, Robins B. 2013. A review of new interpretations of the tectonostratigraphy, geochemistry and evolution of the Onverwacht Suite, Barberton Greenstone Belt, South Africa. Gondwana Res, 23: 403–428

Gaetani G A, Grove T L. 1998. The influence of water on melting of mantle peridotite. Contrib Mineral Petrol, 131: 323–346

Gaetani G A, Grove T L. 2003. Experimental constraints on melt generation in the mantle wedge. Washington D C: American Geophysical Union Geophysical Monograph Series, 138: 107–134

Gaschnig R M, Reinhard C T, Planavsky N J, Wang X, Asael D, Chauvel C. 2017. The molybdenum isotope system as a tracer of slab input in subduction zones: An example from Martinique, Lesser Antilles Arc. Geochem Geophys Geosyst, 18: 4674–4689

Gervasoni F, Klemme S, Rohrbach A, Grützner T, Berndt J. 2017. Experimental constraints on mantle metasomatism caused by silicate and carbonate melts. Lithos, 282-283: 173–186

Gerya T V, Yuen D A. 2003. Rayleigh-Taylor instabilities from hydration and melting propel “cold plumes” at subduction zones. Earth Planet Sci Lett, 212: 47–62

Gill J B. 1981. Orogenic Andesites and Plate Tectonics. New York: Springer-Verlag. 390

Gorman P J, Kerrick D M, Connolly J A D. 2006. Modeling open system metamorphic decarbonation of subducting slabs. Geochem Geophys Geosyst, 7: Q04007

Gorring M, Singer B, Gowers J, Kay S M. 2003. Plio-Pleistocene basalts from the Meseta del Lago Buenos Aires, Argentina: evidence for asthenosphere-lithosphere interactions during slab window magmatism. Chem Geol, 193: 215–235

Green D H. 1973. Experimental melting studies on a model upper mantle composition at high pressure under water-saturated and water-undersaturated conditions. Earth Planet Sci Lett, 19: 37–53

Green D, Ringwood A. 1969. The origin of basalt magmas. Washington D C: American Geophysical Union Geophysical Monograph Series, 13: 489–495

Green D H, Hibberson W O, Kovács I, Rosenthal A. 2010. Water and its influence on the lithosphere-asthenosphere boundary. Nature, 467: 448–451

Green D H, Hibberson W O, Rosenthal A, Kovács I, Yaxley G M, Falloon T J, Brink F. 2014. Experimental study of the influence of water on melting and phase assemblages in the upper mantle. J Petrol, 55: 2067–2096

Green D H, Rosenthal A, Kovács I. 2012. Comment on “The beginnings of hydrous mantle wedge melting”, CB Till, TL Grove, AC Withers, Contributions to Mineralogy and Petrology, DOI 10.1007/s00410-011-0692-6. Contrib Mineral Petrol, 164: 1077–1081

Grove T L, Parman S W, Bowring S A, Price R C, Baker M B. 2002. The role of an H_2O-rich fluid component in the generation of primitive basaltic andesites and andesites from the Mt. Shasta region, N California. Contrib Mineral Petrol, 142: 375–396

Grove T L, Till C B, Krawczynski M J. 2012. The role of H_2O in subduction zone magmatism. Annu Rev Earth Planet Sci, 40: 413–439

Grove T L, Till C B, Lev E, Chatterjee N, Médard E. 2009. Kinematic variables and water transport control the formation and location of arc volcanoes. Nature, 459: 694–697

Grove T, Chatterjee N, Parman S, Médard E. 2006. The influence of H_2O on mantle wedge melting. Earth Planet Sci Lett, 249: 74–89

Gust D A, Perfit M R. 1987. Phase relations of a high-mg basalt from the aleutian island arc: Implications for primary island arc basalts and high-al basalts. Contrib Mineral Petrol, 97: 7–18

Hall P S, Kincaid C. 2001. Diapiric flow at subduction zones: A recipe for rapid transport. Science, 292: 2472–2475

Hamilton W. 1964. Origin of high-alumina basalt, andesite, and dacite magmas. Science, 146: 635–637

Hanyu T, Tatsumi Y, Nakai S. 2002. A contribution of slab-melts to the formation of high-Mg andesite magmas Hf isotopic evidence from Sw Japan. Geophys Res Lett, 29: 2051

Hastie A R, Fitton J G, Mitchell S F, Neill I, Nowell G M, Millar I L. 2015. Can fractional crystallization, mixing and assimilation processes be responsible for Jamaican-type Adakites? Implications for generating Eoarchaean continental crust. J Petrol, 56: 1251–1284

Hawkesworth C J, Gallagher K, Hergt J M, McDermott F. 1993. Mantle and slab contributions in arc magmas. Annu Rev Earth Planet Sci, 21: 175–204

Hermann J, Spandler C J. 2008. Sediment melts at sub-arc depths: An experimental study. J Petrol, 49: 717–740

Hickey-Vargas R, Sun M, Holbik S. 2016. Geochemistry of basalts

from small eruptive centers near Villarrica stratovolcano, Chile: Evidence for lithospheric mantle components in continental arc magmas. Geochim Cosmochim Acta, 185: 358–382

Hirschmann M M, Kogiso T, Baker M B, Stolper E M. 2003. Alkalic magmas generated by partial melting of garnet pyroxenite. Geology, 31: 481–484

Hochstaedter A G, Gill J B, Taylor B, Ishizuka O, Yuasa M, Monta S. 2000. Across-arc geochemical trends in the Izu-Bonin arc: Constraints on source composition and mantle melting. J Geophys Res, 105: 495–512

Hoernle K, Abt D L, Fischer K M, Nichols H, Hauff F, Abers G A, van den Bogaard P, Heydolph K, Alvarado G, Protti M, Strauch W. 2008. Arc-parallel flow in the mantle wedge beneath Costa Rica and Nicaragua. Nature, 451: 1094–1097

Husen A, Almeev R R, Holtz F. 2016. The effect of H_2O and pressure on multiple saturation and liquid lines of descent in basalt from the Shatsky Rise. J Petrol, 57: 309–344

Irving A J, Green D H. 2008. Phase relationships of hydrous alkalic magmas at high pressures: Production of nepheline hawaiitic to mugearitic liquids by amphibole-dominated fractional crystallization within the lithospheric mantle. J Petrol, 49: 741–756

Ishikawa T, Nakamura E. 1994. Origin of the slab component in arc lavas from across-arc variation of B and Pb isotopes. Nature, 370: 205–208

Ishizuka O, Kimura J, Li Y, Stern R, Reagan M, Taylor R, Ohara Y, Bloomer S, Ishii T, Hargroveiii U. 2006. Early stages in the evolution of Izu-Bonin arc volcanism: New age, chemical, and isotopic constraints. Earth Planet Sci Lett, 250: 385–401

Ishizuka O, Tani K, Reagan M K, Kanayama K, Umino S, Harigane Y, Sakamoto I, Miyajima Y, Yuasa M, Dunkley D J. 2011. The timescales of subduction initiation and subsequent evolution of an oceanic island arc. Earth Planet Sci Lett, 306: 229–240

Ishizuka O, Uto K, Yuasa M, Hochstaedter A G. 2003. Volcanism in the earliest stage of back-arc rifting in the izu-bonin arc revealed by laser-heating $^{40}Ar/^{39}Ar$ dating. J Volcanol Geotherm Res, 120: 71–85

Ishizuka O, Yuasa M, Taylor R N, Sakamoto I. 2009. Two contrasting magmatic types coexist after the cessation of back-arc spreading. Chem Geol, 266: 274–296

Johnston A D, Wyllie P J. 1989. The system tonalite-peridotite-H_2O at 30 kbar, with applications to hybridization in subduction zone magmatism. Contrib Mineral Petrol, 102: 257–264

Kawamoto T, Kanzaki M, Mibe K, Matsukage K N, Ono S. 2012. Separation of supercritical slab-fluids to form aqueous fluid and melt components in subduction zone magmatism. Proc Natl Acad Sci USA, 109: 18695–18700

Kay S M, Godoy E, Kurtz A. 2005. Episodic arc migration, crustal thickening, subduction erosion, and magmatism in the south-central andes. Geol Soc Am Bull, 117: 67–88

Kelemen P B, Rilling J L, Parmentier E M, Mehl L, Hacker B R. 2003. Thermal structure due to solid-state flow in the mantle wedge beneath arcs. In: Eiler J, ed. Inside the Subduction Factory. Washington D C: AGU. 293–311

Kelemen P B, Hanghøj K, Greene A R. 2014. One view of the geochemistry of subduction-related magmatic arcs, with an emphasis on primitive andesite and lower crust. In: Turekian K K, ed. Treatise on Geochemistry (Second Edition). Oxford: Elsevier. 749–806

Kepezhinskas P, Defant M J. 1996. Contrasting styles of mantle metasomatism above subduction zones: Constraints from ultramaȼc xenoliths in Kamchatka. In: Bebout G E, Scholl D W, Kirby S H, Platt J P, eds. Subduction: Top to Bottom. Washington D C: AGU. 307–314

Kepezhinskas P K, Defant M J, Drummond M S. 1995. Na metasomatism in the island arc mantle by slab melt-peridotite interaction: Evidence from mantle xenoliths in the North Kamchatka arc. J Petrol, 36: 1505–1527

Kepezhinskas P, McDermott F, Defant M J, Hochstaedter A, Drummond M S, Hawkesworth C J, Koloskov A, Maury R C, Bellon H. 1997. Trace element and Sr-Nd-Pb isotopic constraints on a three-component model of Kamchatka Arc petrogenesis. Geochim Cosmochim Acta, 61: 577–600

Keppler H. 1996. Constraints from partitioning experiments on the composition of subduction-zone fluids. Nature, 380: 237–240

Kessel R, Schmidt M W, Ulmer P, Pettke T. 2005. Trace element signature of subduction-zone fluids, melts and supercritical liquids at 120–180 km depth. Nature, 437: 724–727

Kikuchi Y. 1888. Geological summary of the Bonin and Volcano Islands (in Japanese). Toyo Gakugei-zasshi 5: 64–69

Kikuchi Y. 1890. On pyorxene components in certain volcanic rocks from Bonin Island. J Coll Sci Imp Univ Japan, 3: 67–89

Kimura J I, Ariskin A A. 2014. Calculation of water-bearing primary basalt and estimation of source mantle conditions beneath arcs: Primacalc2 model for windows. Geochem Geophys Geosyst, 15: 1494–1514

Kincaid C, Druken K A, Griffiths R W, Stegman D R. 2013. Bifurcation of the Yellowstone plume driven by subduction-induced mantle flow. Nat Geosci, 6: 395–399

Kincaid C, Griffiths R W. 2003. Laboratory models of the thermal evolution of the mantle during rollback subduction. Nature, 425: 58–62

Kirby S, Engdahl E, Denlinger R. 1996. Intermediate-depth intraplate

earthquakes and arc volcanism as physical expressions of crustal and upper mantle meta-morphism in subducting slabs. In: Bebout G E, Scholl D W, Kirby S H, Platt J P, eds. Subduction Top to Bottom. Washington D C: AGU. 195–214

Klein E M, Langmuir C H. 1987. Global correlations of ocean ridge basalt chemistry with axial depth and crustal thickness. J Geophys Res, 92: 8089–8115

König S, Wille M, Voegelin A, Schoenberg R. 2016. Molybdenum isotope systematics in subduction zones. Earth Planet Sci Lett, 447: 95–102

Konrad-Schmolke M, Halama R, Manea V C. 2016. Slab mantle dehydrates beneath Kamchatka-yet recycles water into the deep mantle. Geochem Geophys Geosyst, 17: 2987–3007

Korenaga J, Kelemen P B. 2000. Major element heterogeneity in the mantle source of the North Atlantic igneous province. Earth Planet Sci Lett, 184: 251–268

Kuno H. 1960. High-alumina basalt. J Petrol, 1: 121–145

Kuritani T, Yokoyama T, Nakamura E. 2008. Generation of rear-arc magma induced by influx of slab-derived supercritical liquids: Implications from alkali basalt lavas from Rishiri Volcano, Kurile arc. J Petrol, 49: 1319–1342

Kushiro I. 1959. Preliminary note on alkali-dolerite of atumi district, northern Japan. Jap J Geol Geogr, 30: 259–272

Kushiro I. 1968. Compositions of magmas formed by partial zone melting of the Earth's upper mantle. J Geophys Res, 73: 619–634

Lai Y M, Song S R, Lo C H, Lin T H, Chu M F, Chung S L. 2017. Age, geochemical and isotopic variations in volcanic rocks from the Coastal Range of Taiwan: Implications for magma generation in the Northern Luzon Arc. Lithos, 272-273: 92–115

Lambart S, Laporte D, Provost A, Schiano P. 2012. Fate of pyroxenite-derived melts in the peridotitic mantle: Thermodynamic and experimental constraints. J Petrol, 53: 451–476

Lambart S, Laporte D, Schiano P. 2009. An experimental study of pyroxenite partial melts at 1 and 1.5 GPa: Implications for the major-element composition of Mid-Ocean ridge basalts. Earth Planet Sci Lett, 288: 335–347

Le Voyer M, Rose-Koga E F, Shimizu N, Grove T L, Schiano P. 2010. Two contrasting H_2O-rich components in primary melt inclusions from mount shasta. J Petrol, 51: 1571–1595

Leeman W P, Lewis J F, Evarts R C, Conrey R M, Streck M J. 2005. Petrologic constraints on the thermal structure of the Cascades arc. J Volcanol Geotherm Res, 140: 67–105

Leslie R A J, Danyushevsky L V, Crawford A J, Verbeeten A C. 2009. Primitive shoshonites from Fiji: Geochemistry and source components. Geochem Geophys Geosyst, 10: Q07001

Li H Y, Taylor R N, Prytulak J, Kirchenbaur M, Shervais J W, Ryan J G, Godard M, Reagan M K, Pearce J A. 2019. Radiogenic isotopes document the start of subduction in the Western Pacific. Earth Planet Sci Lett, 518: 197–210

Lin P N, Stern R J, Bloomer S H. 1989. Shoshonitic volcanism in the northern Mariana arc: 2. Large-ion lithophile and rare earth element abundances: Evidence for the source of incompatible element enrichments in intraoceanic arcs. J Geophys Res, 94: 4497–4514

Liu L, Stegman D R. 2012. Origin of Columbia River flood basalt controlled by propagating rupture of the Farallon slab. Nature, 482: 386–389

Lynn K J, Shea T, Garcia M O, Costa F, Norman M D. 2018. Lithium diffusion in olivine records magmatic priming of explosive basaltic eruptions. Earth Planet Sci Lett, 500: 127–135

Mallik A, Dasgupta R, Tsuno K, Nelson J. 2016. Effects of water, depth and temperature on partial melting of mantle-wedge fluxed by hydrous sediment-melt in subduction zones. Geochim Cosmochim Acta, 195: 226–243

Mallik A, Dasgupta R. 2012. Reaction between MORB-eclogite derived melts and fertile peridotite and generation of ocean island basalts. Earth Planet Sci Lett, 329-330: 97–108

Mallik A, Nelson J, Dasgupta R. 2015. Partial melting of fertile peridotite fluxed by hydrous rhyolitic melt at 2–3 GPa: Implications for mantle wedge hybridization by sediment melt and generation of ultrapotassic magmas in convergent margins. Contrib Mineral Petrol, 169: 48

Manning C E. 2004. The chemistry of subduction-zone fluids. Earth Planet Sci Lett, 223: 1–16

Marschall H R, Schumacher J C. 2012. Arc magmas sourced from mélange diapirs in subduction zones. Nat Geosci, 5: 862–867

Martin C, Flores K E, Harlow G E. 2016. Boron isotopic discrimination for subduction-related serpentinites. Geology, 44: 899–902

Martin H, Moyen J F, Guitreau M, Blichert-Toft J, Le Pennec J L. 2014. Why Archaean TTG cannot be generated by MORB melting in subduction zones. Lithos, 198-199: 1–13

Martin H, Smithies R H, Rapp R, Moyen J F, Champion D. 2005. An overview of adakite, tonalite-trondhjemite-granodiorite (TTG), and sanukitoid: Relationships and some implications for crustal evolution. Lithos, 79: 1–24

McGary R S, Evans R L, Wannamaker P E, Elsenbeck J, Rondenay S. 2014. Pathway from subducting slab to surface for melt and fluids beneath Mount Rainier. Nature, 511: 338–340

McInnes B I A, Gregoire M, Binns R A, Herzig P M, Hannington M D. 2001. Hydrous metasomatism of oceanic sub-arc mantle, Lihir, Papua New Guinea: Petrology and geochemistry of fluid-metasomatised mantle wedge xenoliths. Earth Planet Sci Lett, 188: 169–183

Médard E, Schmidt M W, Schiano P, Ottolini L. 2006. Melting of

amphibole-bearing wehrlites: An experimental study on the origin of ultra-calcic nepheline-normative melts. J Petrol, 47: 481–504

Meffre S, Falloon T J, Crawford T J, Hoernle K, Hauff F, Duncan R A, Bloomer S H, Wright D J. 2012. Basalts erupted along the tongan fore arc during subduction initiation: Evidence from geochronology of dredged rocks from the tonga fore arc and trench. Geochem Geophys Geosyst, 13: Q12003

Melekhova E, Blundy J, Robertson R, Humphreys M C S. 2015. Experimental evidence for polybaric differentiation of primitive arc basalt beneath St. Vincent, Lesser Antilles. J Petrol, 56: 161–192

Mibe K, Kawamoto T, Matsukage K N, Fei Y, Ono S. 2011. Slab melting versus slab dehydration in subduction-zone magmatism. Proc Natl Acad Sci USA, 108: 8177–8182

Morgan Z, Liang Y. 2003. An experimental and numerical study of the kinetics of harzburgite reactive dissolution with applications to dunite dike formation. Earth Planet Sci Lett, 214: 59–74

Moriguti T, Nakamura E. 1998. Across-arc variation of Li isotopes in lavas and implications for crust/mantle recycling at subduction zones. Earth Planet Sci Lett, 163: 167–174

Morrison G W. 1980. Characteristics and tectonic setting of the shoshonite rock association. Lithos, 13: 97–108

Mullen E K, Weis D, Marsh N B, Martindale M. 2017. Primitive arc magma diversity: New geochemical insights in the cascade arc. Chem Geol, 448: 43–70

Mullen E K, Weis D. 2013. Sr-Nd-Hf-Pb isotope and trace element evidence for the origin of alkalic basalts in the Garibaldi Belt, northern Cascade arc. Geochem Geophys Geosyst, 14: 3126–3155

Müller D, Franz L, Herzig P M, Hunt S. 2001. Potassic igneous rocks from the vicinity of epithermal gold mineralization, Lihir Island, Papua New Guinea. Lithos, 57: 163–186

Müller D, Rock N M S, Groves D I. 1992. Geochemical discrimination between shoshonitic and potassic volcanic rocks in different tectonic settings: A pilot study. Mineral Petrol, 46: 259–289

Nakajima J, Hasegawa A. 2007. Subduction of the philippine sea plate beneath southwestern japan: Slab geometry and its relationship to arc magmatism. J Geophys Res, 112: B08306

Ni H, Zhang L, Xiong X, Mao Z, Wang J. 2017. Supercritical fluids at subduction zones: Evidence, formation condition, and physico-chemical properties. Earth-Sci Rev, 167: 62–71

Nicholls I A, Ringwood A E. 1973. Production of silica-saturated tholeiitic magmas in island arcs. Earth Planet Sci Lett, 17: 243–246

Nielsen S G, Marschall H R. 2017. Geochemical evidence for mélange melting in global arcs. Sci Adv, 3: e1602402

Niu Y. 2005. Generation and evolution of basaltic magmas: Some basic concepts and a new view on the origin of Mesozoic-Cenozoic basaltic volcanism in eastern China. Geol J China Univ, 11: 9–46

Pabst S, Zack T, Savov I P, Ludwig T, Rost D, Vicenzi E P. 2011. Evidence for boron incorporation into the serpentine crystal structure. Am Miner, 96: 1112–1119

Parman S W, Grove T L, Kelley K A, Plank T. 2011. Along-arc variations in the pre-eruptive H_2O contents of Mariana Arc magmas inferred from fractionation paths. J Petrol, 52: 257–278

Peacock S M, Rushmer T, Thompson A B. 1994. Partial melting of subducting oceanic crust. Earth Planet Sci Lett, 121: 227–244

Peate D W, Pearce J A, Hawkesworth C J, Colley H, Edwards C M H, Hirose K. 1997. Geochemical variations in vanuatu arc lavas: The role of subducted material and a variable mantle wedge composition. J Petrol, 38: 1331–1358

Pertermann M, Hirschmann M M. 2003. Partial melting experiments on a MORB-like pyroxenite between 2 and 3 GPa: Constraints on the presence of pyroxenite in basalt source regions from solidus location and melting rate. J Geophys Res, 108: 2125

Pichavant M, MacDonald R. 2007. Crystallization of primitive basaltic magmas at crustal pressures and genesis of the calc-alkaline igneous suite: Experimental evidence from St Vincent, Lesser Antilles arc. Contrib Mineral Petrol, 154: 535–558

Pilet S, Baker M B, Stolper E M. 2008. Metasomatized lithosphere and the origin of alkaline lavas. Science, 320: 916–919

Pirard C, Hermann J. 2015. Focused fluid transfer through the mantle above subduction zones. Geology, 43: 915–918

Plank T, Kelley K A, Zimmer M M, Hauri E H, Wallace P J. 2013. Why do mafic arc magmas contain ~4 wt% water on average? Earth Planet Sci Lett, 364: 168–179

Plank T, Langmuir C H. 1988. An evaluation of the global variations in the major element chemistry of arc basalts. Earth Planet Sci Lett, 90: 349–370

Polat A, Kerrich R. 2002. Nd-isotope systematics of ~2.7 Ga adakites, magnesian andesites, and arc basalts, Superior Province: Evidence for shallow crustal recycling at Archean subduction zones. Earth Planet Sci Lett, 202: 345–360

Price A A, Jackson M G, Blichert-Toft J, Hall P S, Sinton J M, Kurz M D, Blusztajn J. 2014. Evidence for a broadly distributed Samoan-plume signature in the northern Lau and North Fiji Basins. Geochem Geophys Geosyst, 15: 986–1008

Prigent C, Guillot S, Agard P, Lemarchand D, Soret M, Ulrich M. 2018. Transfer of subduction fluids into the deforming mantle wedge during nascent subduction: Evidence from trace elements and boron isotopes (Semail ophiolite, Oman). Earth Planet Sci Lett, 484: 213–228

Rapp R P, Shimizu N, Norman M D, Applegate G S. 1999. Reaction between slab-derived melts and peridotite in the mantle wedge: Experimental constraints at 3.8 GPa. Chem Geol, 160: 335–356

Rapp R P, Watson E B. 1995. Dehydration Melting of Metabasalt at 8–32 kbar: Implications for Continental Growth and Crust-Mantle Recycling. J Petrol, 36: 891–931

Reagan M K, Ishizuka O, Stern R J, Kelley K A, Ohara Y, Blichert-Toft J, Bloomer S H, Cash J, Fryer P, Hanan B B, Hickey-Vargas R, Ishii T, Kimura J I, Peate D W, Rowe M C, Woods M. 2010. Fore-arc basalts and subduction initiation in the Izu-Bonin-Mariana system. Geochem Geophys Geosyst, 11: Q03X12

Ringwood A E. 1990. Slab-mantle interactions. Chem Geol, 82: 187–207

Ringwood A E. 1974. The petrological evolution of island arc systems. J Geol Soc, 130: 183–204

Roeder P L, Emslie R F. 1970. Olivine-liquid equilibrium. Contrib Mineral Petrol, 29: 275–289

Rogers N. 2015. The composition and origin of magmas. In: Sigurdsson H, Houghton B F, Mcnutt S R, Rymer H, Stix J, Mcbirney A R, eds. The Encyclopedia of Volcanoes. London: Academic Press. 93–112

Ruprecht P, Plank T. 2013. Feeding andesitic eruptions with a high-speed connection from the mantle. Nature, 500: 68–72

Ruth D C S, Costa F, Bouvet de Maisonneuve C, Franco L, Cortés J A, Calder E S. 2018. Crystal and melt inclusion timescales reveal the evolution of magma migration before eruption. Nat Commun, 9: 2657

Sajona F G, Bellon H, Maury R C, Pubellier M, Cotten J, Rangin C. 1994. Magmatic response to abrupt changes in geodynamic settings: Pliocene—Quaternary calc-alkaline and Nb-enriched lavas from Mindanao (Philippines). Tectonophysics, 237: 47–72

Sajona F G, Maury R C, Bellon H, Cotten J, Defant M. 1996. High field strength element enrichment of Pliocene-Pleistocene Island arc basalts, Zamboanga Peninsula, western Mindanao (Philippines). J Petrol, 37: 693–726

Sajona F G, Maury R C, Bellon H, Cotten J, Defant M J, Pubellier M. 1993. Initiation of subduction and the generation of slab melts in Western and Eastern Mindanao, Philippines. Geology, 21: 1007–1010

Sano Y, Williams S N. 1996. Fluxes of mantle and subducted carbon along convergent plate boundaries. Geophys Res Lett, 23: 2749–2752

Saper L, Liang Y. 2014. Formation of plagioclase-bearing peridotite and plagioclase-bearing wehrlite and gabbro suite through reactive crystallization: An experimental study. Contrib Mineral Petrol, 167: 985

Savov I P, Ryan J G, D'Antonio M, Fryer P. 2007. Shallow slab fluid release across and along the Mariana arc-basin system: Insights from geochemistry of serpentinized peridotites from the Mariana fore arc. J Geophys Res, 112: B09205

Savov I P, Ryan J G, D'Antonio M, Kelley K, Mattie P. 2005. Geochemistry of serpentinized peridotites from the Mariana Forearc Conical Seamount, ODP Leg 125: Implications for the elemental recycling at subduction zones. Geochem Geophys Geosyst, 6: Q04J15

Scambelluri M, Tonarini S. 2012. Boron isotope evidence for shallow fluid transfer across subduction zones by serpentinized mantle. Geology, 40: 907–910

Scherbarth N L, Spry P G. 2006. Mineralogical, petrological, stable isotope, and fluid inclusion characteristics of the tuvatu gold-silver telluride deposit, Fiji: Comparisons with the emperor deposit. Econ Geol, 101: 135–158

Schmidt M W. 1996. Experimental constraints on recycling of potassium from subducted oceanic crust. Science, 272: 1927–1930

Schmidt M W. 2015. Melting of pelitic sediments at subarc depths: 2. Melt chemistry, viscosities and a parameterization of melt composition. Chem Geol, 404: 168–182

Schmidt M W, Jagoutz O. 2017. The global systematics of primitive arc melts. Geochem Geophys Geosyst, 18: 2817–2854

Schmidt M W, Poli S. 1998. Experimentally based water budgets for dehydrating slabs and consequences for arc magma generation. Earth Planet Sci Lett, 163: 361–379

Schmidt M W, Poli S. 2014. 4.19. Devolatilization during subduction. In: Turekian K K, ed. Treatise on Geochemistry (Second Edition). Oxford: Elsevier. 669–697

Scholl D W, Plank T, Morris J, von Huene R, Mottl M J. 1994. Science opportunities in Ocean Drilling to investigate recycling processes and material fluxes at subduction zones. Avalon: Proceedings of a JOI/USSAC workshop

Schuth S, Münker C, König S, Qopoto C, Basi S, Garbe-Schönberg D, Ballhaus C. 2009. Petrogenesis of lavas along the solomon island arc, sw pacific: Coupling of compositional variations and subduction zone geometry. J Petrol, 50: 781–811

Shervais J W, Reagan M, Haugen E, Almeev R R, Pearce J A, Prytulak J, Ryan J G, Whattam S A, Godard M, Chapman T, Li H, Kurz W, Nelson W R, Heaton D, Kirchenbaur M, Shimizu K, Sakuyama T, Li Y, Vetter S K. 2019. Magmatic response to subduction initiation: Part 1. Fore-arc basalts of the Izu-Bonin Arc From IODP expedition 352. Geochem Geophys Geosyst, 20: 314–338

Shirey S B, Hanson G N. 1984. Mantle-derived Archaean monzodiorites and trachyandesites. Nature, 310: 222–224

Shuto K, Nohara-Imanaka R, Sato M, Takahashi T, Takazawa E, Kawabata H, Takanashi K, Ban M, Watanabe N, Fujibayashi N. 2015. Across-arc variations in geochemistry of oligocene to quaternary basalts from the ne japan arc: Constraints on source composition, mantle melting and slab input composition. J Petrol,

56: 2257–2297

Sisson T W, Grove T L. 1993. Experimental investigations of the role of H_2O in calc-alkaline differentiation and subduction zone magmatism. Contrib Mineral Petrol, 113: 143–166

Sisson T W, Kelemen P B. 2018. Near-solidus melts of MORB + 4 wt% H_2O at 0.8–2.8 GPa applied to issues of subduction magmatism and continent formation. Contrib Mineral Petrol, 173: 70

Sisson T W, Layne G D. 1993. H2O in basalt and basaltic andesite glass inclusions from four subduction-related volcanoes. Earth Planet Sci Lett, 117: 619–635

Smithies R H, Champion D C, Sun S S. 2004. Evidence for Early LREE-enriched mantle source regions: Diverse Magmas from the c. 3.0 Ga Mallina Basin, Pilbara Craton, NW Australia. J Petrol, 45: 1515–1537

Smithies R H, Champion D C, Cassidy K F. 2003. Formation of Earth's early Archaean continental crust. Precambrian Res, 127: 89–101

Sorbadere F, Médard E, Laporte D, Schiano P. 2013a. Experimental melting of hydrous peridotite-pyroxenite mixed sources: Constraints on the genesis of silica-undersaturated magmas beneath volcanic arcs. Earth Planet Sci Lett, 384: 42–56

Sorbadere F, Schiano P, Métrich N, Bertagnini A. 2013b. Small-scale coexistence of island-arc- and enriched-MORB-type basalts in the central Vanuatu arc. Contrib Mineral Petrol, 166: 1305–1321

Spandler C, Pirard C. 2013. Element recycling from subducting slabs to arc crust: A review. Lithos, 170-171: 208–223

Spandler C, Yaxley G, Green D H, Scott D. 2010. Experimental phase and melting relations of metapelite in the upper mantle: Implications for the petrogenesis of intraplate magmas. Contrib Mineral Petrol, 160: 569–589

Stalder R, Foley S F, Brey G P, Horn I. 1998. Mineral-aqueous fluid partitioning of trace elements at 900–1200°C and 3.0–5.7 GPa: New experimental data for garnet, clinopyroxene, and rutile, and implications for mantle metasomatism. Geochim Cosmochim Acta, 62: 1781–1801

Stern R J. 2010. The anatomy and ontogeny of modern intra-oceanic arc systems. Geol Soc Lond Spec Publ, 338: 7–34

Straub S M, Gómez-Tuena A, Bindeman I N, Bolge L L, Brandl P A, Espinasa-Perena R, Solari L, Stuart F M, Vannucchi P, Zellmer G F. 2015. Crustal recycling by subduction erosion in the central mexican volcanic belt. Geochim Cosmochim Acta, 166: 29–52

Su B X, Zhou M F, Robinson P T. 2016. Extremely large fractionation of Li isotopes in a chromitite-bearing mantle sequence. Sci Rep, 6: 22370

Su B, Chen Y, Guo S, Chen S, Li Y. 2019. Garnetite and pyroxenite in the mantle wedge formed by slab-mantle interactions at different melt/rock ratios. J Geophys Res Solid Earth, 124: 6504–6522

Sun S, McDonough W F. 1989. Chemical and isotopic systematics of oceanic basalts: Implications for mantle composition and processes. Geol Soc Lond Spec Publ, 42: 313–345

Syracuse E M, van Keken P E, Abers G A, Suetsugu D, Bina C, Inoue T, Wiens D, Jellinek M. 2010. The global range of subduction zone thermal models. Phys Earth Planet Inter, 183: 73–90

Tamura A, Arai S. 2006. Harzburgite-dunite-orthopyroxenite suite as a record of supra-subduction zone setting for the Oman ophiolite mantle. Lithos, 90: 43–56

Tang G J, Wang Q, Wyman D, Sun M, Li Z X, Zhao Z H, Sun W D, Jia X H, Jiang Z Q. 2010. Geochronology and geochemistry of Late Paleozoic magmatic rocks in the Lamasu-Dabate area, northwestern Tianshan (west China): Evidence for a tectonic transition from arc to post-collisional setting. Lithos, 119: 3–4

Tang M, Rudnick R L, Chauvel C. 2014. Sedimentary input to the source of Lesser Antilles lavas: A Li perspective. Geochim Cosmochim Acta, 144: 43–58

Tatsumi Y, Hamilton D L, Nesbitt R W. 1986. Chemical characteristics of fluid phase released from a subducted lithosphere and origin of arc magmas: Evidence from high-pressure experiments and natural rocks. J Volcanol Geotherm Res, 29: 293–309

Tatsumi Y, Kogiso T. 2003. The subduction factory: Its role in the evolution of the earth's crust and mantle. Geol Soc Lond Spec Publ, 219: 55–80

Tatsumi Y, Sakuyama M, Fukuyama H, Kushiro I. 1983. Generation of arc basalt magmas and thermal structure of the mantle wedge in subduction zones. J Geophys Res, 88: 5815–5825

Tatsumi Y, Takahashi T, Hirahara Y, Chang Q, Miyazaki T, Kimura J I, Ban M, Sakayori A. 2008. New insights into andesite genesis: The role of mantle-derived calc-alkalic and crust-derived tholeiitic melts in magma differentiation beneath zao volcano, NE Japan. J Petrol, 49: 1971–2008

Tatsumi Y. 1989. Migration of fluid phases and genesis of basalt magmas in subduction zones. J Geophys Res, 94: 4697–4707

Tatsumi Y. 2005. The subduction factory: How it operates in the evolving earth. GSA Today, 15: 4–10

Tatsumi Y. 2006. High-mg andesites in the setouchi volcanic belt, southwestern japan: Analogy to archean magmatism and continental crust formation? Annu Rev Earth Planet Sci, 34: 467–499

Teng F Z, Hu Y, Chauvel C. 2016. Magnesium isotope geochemistry in arc volcanism. Proc Natl Acad Sci USA, 113: 7082–7087

Tenner T J, Hirschmann M M, Humayun M. 2012. The effect of H_2O on partial melting of garnet peridotite at 3.5 GPa. Geochem Geophys Geosyst, 13: Q03016

Thomsen T B, Schmidt M W. 2008. Melting of carbonated pelites at 2.5–5.0 GPa, silicate-carbonatite liquid immiscibility, and potas-

sium-carbon metasomatism of the mantle. Earth Planet Sci Lett, 267: 17–31

Thomson A R, Walter M J, Kohn S C, Brooker R A. 2016. Slab melting as a barrier to deep carbon subduction. Nature, 529: 76–79

Thorkelson D J, Madsen J K, Sluggett C L. 2011. Mantle flow through the Northern Cordilleran slab window revealed by volcanic geochemistry. Geology, 39: 267–270

Till C B, Grove T L, Withers A C. 2012. The beginnings of hydrous mantle wedge melting. Contrib Mineral Petrol, 163: 669–688

Tomita T. 1935. On the chemical composition of the Cenozoic alkaline suite of the circum-japan sea region. J Shanghai Sci Inst, 1: 227–306

Tonarini S, Leeman W P, Leat P T. 2011. Subduction erosion of forearc mantle wedge implicated in the genesis of the South Sandwich Island (SSI) arc: Evidence from boron isotope systematics. Earth Planet Sci Lett, 301: 275–284

Tsuno K, Dasgupta R. 2011. Melting phase relation of nominally anhydrous, carbonated pelitic-eclogite at 2.5–3.0 GPa and deep cycling of sedimentary carbon. Contrib Mineral Petrol, 161: 743–763

Tsuno K, Dasgupta R. 2012. The effect of carbonates on near-solidus melting of pelite at 3 GPa: Relative efficiency of H_2O and CO_2 subduction. Earth Planet Sci Lett, 319-320: 185–196

Turner S, Rushmer T, Reagan M, Moyen J F. 2014. Heading down early on? Start of subduction on Earth. Geology, 42: 139–142

Turner S J, Langmuir C H, Dungan M A, Escrig S. 2017. The importance of mantle wedge heterogeneity to subduction zone magmatism and the origin of EM1. Earth Planet Sci Lett, 472: 216–228

Tursack E, Liang Y. 2012. A comparative study of melt-rock reactions in the mantle: Laboratory dissolution experiments and geological field observations. Contrib Mineral Petrol, 163: 861–876

Ulmer P, Trommsdorff V. 1995. Serpentine stability to mantle depths and subduction-related magmatism. Science, 268: 858–861

Van den Bleeken G, Muntener O, Ulmer P. 2010. Reaction processes between tholeiitic melt and residual peridotite in the uppermost mantle: An experimental study at 0.8 GPa. J Petrol, 51: 153–183

Van den Bleeken G, Müntener O, Ulmer P. 2011. Melt variability in percolated peridotite: An experimental study applied to reactive migration of tholeiitic basalt in the upper mantle. Contrib Mineral Petrol, 161: 921–945

Varfalvy V, Hébert R, Bedard J H. 1996. Interactions between melt and upper-mantle peridotites in the north arm mountain massif, Bay of islands ophiolite, Newfoundland, Canada: Implications for the genesis of boninitic and related magmas. Chem Geol, 129: 71–90

Villiger S, Ulmer P, Müntener O, Thompson A B. 2004. The liquid line of descent of anhydrous, mantle-derived, tholeiitic liquids by fractional and equilibrium crystallization—An experimental study at 1.0 GPa. J Petrol, 45: 2369–2388

Wallace P J. 2005. Volatiles in subduction zone magmas: Concentrations and fluxes based on melt inclusion and volcanic gas data. J Volcanol Geotherm Res, 140: 217–240

Wang C G, Liang Y, Dygert N, Xu W L. 2016. Formation of orthopyroxenite by reaction between peridotite and hydrous basaltic melt: An experimental study. Contrib Mineral Petrol, 171: 77

Wang C G, Liang Y, Xu W L, Dygert N. 2013. Effect of melt composition on basalt and peridotite interaction: Laboratory dissolution experiments with applications to mineral compositional variations in mantle xenoliths from the North China Craton. Contrib Mineral Petrol, 166: 1469–1488

Wang M L, Zang C J, Tang H F. 2019. The effect of *P-T* on the reaction between tonalitic melt and mantle lherzolite at 2–4 GPa and implications for evolution of North China Cratonic Lithosphere and generation of High $Mg^{\#}$ andesite. Lithos, 324-325: 626–639

Wang Q, Wyman A, Xu J F, Wan Y S, Li C F, Zi F, Jiang Z Q, Qiu H N, Chu Z Y, Zhao Z H, Dong Y H. 2008. Triassic Nb-enriched basalts, magnesian andesites, and adakites of the Qiangtang terrane (Central Tibet): Evidence for metasomatism by slab-derived melts in the mantle wedge. Contrib Mineral Petrol, 155: 473–490

Wang Q, Wyman D A, Zhao Z H, Xu J F, Bai Z H, Xiong X L, Dai T M, Li C F, Chu Z Y. 2007. Petrogenesis of Carboniferous adakites and Nb-enriched arc basalts in the Alataw area, northern Tianshan Range (western China): Implications for Phanerozoic crustal growth in the Central Asia orogenic belt. Chem Geol, 236: 42–64

Whattam S A. 2018. Primitive magmas in the early Central American volcanic arc system generated by plume-induced subduction initiation. Front Earth Sci, 6: 114

Williams H M, Prytulak J, Woodhead J D, Kelley K A, Brounce M, Plank T. 2018. Interplay of crystal fractionation, sulfide saturation and oxygen fugacity on the iron isotope composition of arc lavas: An example from the Marianas. Geochim Cosmochim Acta, 226: 224–243

Wilson M. 1989. Igneous Petrogenesis. Berlin: Springer

Winter J D. 2014. Principles of Igneous and Metamorphic Petrology. Essex: Pearson Education

Wolfe R C, Cooke D R. 2011. Geology of the didipio region and genesis of the dinkidi alkalic porphyry Cu-Au deposit and related pegmatites, northern luzon, philippines. Econ Geol, 106: 1279–1315

Woodland A B, Bulatov V K, Brey G P, Girnis A V, Höfer H E, Gerdes A. 2018. Subduction factory in an ampoule: Experiments on sediment-peridotite interaction under temperature gradient conditions. Geochim Cosmochim Acta, 223: 319–349

Xia X H, Song S G, Niu Y L. 2012. Tholeiite-Boninite terrane in the North Qilian suture zone: Implications for subduction initiation and back-arc basin development. Chem Geol, 328: 259–277

Xie W, Xu Y G, Chen Y B, Luo Z Y, Hong L B, Ma L, Liu H Q. 2016. High-alumina basalts from the Bogda Mountains suggest an arc setting for Chinese Northern Tianshan during the Late Carboniferous. Lithos, 256-257: 165–181

Xu Y G, Ma J L, Huang X L, Iizuka Y, Chung S L, Wang Y B, Wu X Y. 2004. Early Cretaceous gabbroic complex from Yinan, Shandong Province: Petrogenesis and mantle domains beneath the North China Craton. Int J Earth Sci-Geol Rundsch, 93: 1025–1041

Yoder H S, Tilley C E. 1962. Origin of basalt magmas: An experimental study of natural and synthetic rock systems. J Petrol, 3: 342–532

Zhang Y Y, Yuan C, Sun M, Long X P, Wang Y P, Jiang Y D, Lin Z F. 2017. Arc magmatism associated with steep subduction: Insights from trace element and Sr-Nd-Hf-B isotope systematics. J Geophys Res Solid Earth, 122: 1816–1834

Zheng Y F. 2019. Subduction zone geochemistry. Geosci Front, 10: 1223–1254

Zheng Y F, Xu Z, Chen L, Dai L Q, Zhao Z F. 2020. Chemical geodynamics of mafic magmatism above subduction zones. J Asian Earth Sci, 194: 104185

Zhu G, Gerya T V, Yuen D A, Honda S, Yoshida T, Connolly J A D. 2009. Three-dimensional dynamics of hydrous thermal-chemical plumes in oceanic subduction zones. Geochem Geophys Geosyst, 10: Q11006

Zimmer M M, Plank T, Hauri E H, Yogodzinski G M, Stelling P, Larsen J, Singer B, Jicha B, Mandeville C, Nye C J. 2010. The role of water in generating the calc-alkaline trend: New volatile data for Aleutian magmas and a new tholeiitic index. J Petrol, 51: 2411–2444

(责任编委: 郑永飞)